HHS Public Access

Author manuscript

Pflugers Arch. Author manuscript; available in PMC 2017 May 01.

Published in final edited form as:

Pflugers Arch. 2016 May ; 468(5): 775–793. doi:10.1007/s00424-015-1780-7.

Cross-signaling in metabotropic glutamate 2 and serotonin 2A receptor heteromers in mammalian cells

Lia Baki[1], **Miguel Fribourg**[2], **Jason Younkin**[1], **Jose Miguel Eltit**[1], **Jose L. Moreno**[3], **Gyu Park**[1], **Zhanna Vysotskaya**[1], **Adishesh Narahari**[1], **Stuart C. Sealfon**[2,4,5], **Javier Gonzalez-Maeso**[1,2,3,5], and **Diomedes E. Logothetis**[1,*]

[1]Department of Physiology and Biophysics, Virginia Commonwealth University School of Medicine, Richmond, Virginia 23298, USA

[2]Department of Neurology, Icahn School of Medicine at Mount Sinai, New York, New York 10029, USA

[3]Department of Psychiatry, Icahn School of Medicine at Mount Sinai, New York, New York 10029, USA

[4]Department of Neuroscience, Icahn School of Medicine at Mount Sinai, New York, New York 10029, USA

[5]Friedman Brain Institute, Icahn School of Medicine at Mount Sinai, New York, New York 10029, USA

Abstract

We previously reported that co-expression of the Gi-coupled metabotropic glutamate receptor 2 ($mGlu_2R$) and the Gq-coupled serotonin (5-HT) 2A receptor (2AR) in *Xenopus* oocytes (Fribourg et al., 2011) results in inverse cross-signaling, where for either receptor, strong agonists suppress and inverse agonists potentiate the signaling of the partner receptor. Importantly, through this cross-signaling, the $mGlu_2R$/2AR heteromer integrates the actions of psychotropic and antipsychotic drugs. To investigate whether $mGlu_2R$ and 2AR can cross-signal in mammalian cells, we stably co-expressed them in HEK293 cells along with the GIRK1/GIRK4 channel, a reporter of Gi and Gq signaling activity. Crosstalk-positive clones were identified by Fura-2 calcium imaging, based on potentiation of 5-HT-induced Ca^{2+} responses by the inverse $mGlu_{2/3}R$ agonist LY341495. Cross signaling from both sides of the complex was confirmed in representative clones by using the GIRK channel reporter, both in whole-cell patch-clamp and in fluorescence assays using potentiometric dyes, and further established by competition binding assays. Notably, only 25–30% of the clones were crosstalk positive. The crosstalk-positive phenotype correlated with a) increased colocalization of the two receptors at the cell surface, b) lower density of $mGlu_2R$ binding sites and higher density of 2AR binding sites in total membrane preparations, and c) higher ratios of $mGlu_2R$/2AR normalized surface protein expression. Consistent with our results in *Xenopus* oocytes, a combination of ligands targeting both receptors could elicit functional crosstalk in a crosstalk-negative clone. Crosstalk-positive clones can be

*Correspondence: Diomedes E. Logothetis, delogothetis@vcu.edu, 804-828-5878 (tel), 804-628-3501 (fax).

used in high-throughput assays for identification of antipsychotic drugs targeting this receptor heterocomplex.

Keywords

G protein-coupled receptor (GPCR); metabotropic glutamate 2 ($mGlu_2$) receptor; 5-HT2A receptor; cross-signaling; calcium intracellular release; membrane potential probes; mammalian cells

Introduction

Heteromerization of G protein-coupled receptors (GPCRs) is increasingly appreciated as a mechanism for diversifying GPCR responses, allowing fine-tuning in a cell-type specific manner. GPCR heteromers often have distinct functional properties compared to their constituent protomers. Heteromerization can be critical for the formation of a functional receptor from two non-functional protomers, as in the case of $GABA_B$ receptors where hetero-dimerization between the $GABA_BR1$ and $GABA_BR2$ is required for receptor function [17,19,42]. In other cases heteromerization appears to be important for allosteric regulation and fine-tuning of receptor signaling. Examples are the existence of heteromer-specific pharmacological profiles, as in the case of heteromers between κ and δ [18] and between μ and δ opioid receptors [12]; the quantitative changes of the signaling properties of the complex as in the cases of heteromers formed by the Adenosine 1/Dopamine 1 receptors (A1R–D1R) [10] and the serotonin 2A (2AR)/ /dopamine 2 receptors (2AR/D2R) [1]; the ligand-induced conformational coupling of the μ opioid with the alpha 2 adrenergic receptor ($ADR_{\alpha 2A}$) [39]. In the central nervous system this integration of signaling through allosteric receptor-receptor interactions provides signaling diversity by allowing a given neurotransmitter to trigger qualitatively or quantitatively different downstream responses in neurons expressing different heteromeric complexes [9,1,35].

The Gq-coupled $5\text{-}HT2_A$ receptor (2AR) and the Gi-coupled metabotropic glutamate receptor 2 ($mGlu_2R$) are two neurotransmitter GPCRs implicated in psychosis. The former is involved in the mechanism of action of atypical antipsychotic drugs, acting as its antagonists/inverse agonists, and those of hallucinogens acting as strong agonists. Evidence associating $mGlu_2R$ with psychosis comes from the antipsychotic effects of strong agonists targeting group II metabotropic glutamate receptors [30,21] and from behavioral studies showing that $mGlu_2R$, but not the closely related $mGlu_3R$, mediates these antipsychotic-like effects in experimental models of psychosis [8,36,43]. The $mGlu_2$ and 2A receptors form heteromers in heterologous expression systems as well as in mouse and human frontal cortex [13,29,28]. The physiological significance of this complex is highlighted by behavioral experiments demonstrating that in experimental models of psychosis the antipsychotic-like effects of drugs targeting either receptor require the presence of the partner receptor [11] and that wild-type $mGlu_2R$, but not a mutant unable to bind 2AR, can rescue the head-twitch behavior induced by the hallucinogenic $5\text{-}HT2_A$ receptor agonist DOI [29].

We recently reported that formation of the $mGlu_2R$/2AR heterocomplex in *Xenopus* oocytes introduces an inverse relationship in the active/inactive conformations and signaling

properties of the two receptors, altering the balance between Gi and Gq signaling [11]. In response to the natural ligands glutamate and serotonin, In response to the natural ligands glutamate and serotonin, heterocomplex formation enhances Gi signaling through $mGlu_2R$ and reduces Gq signaling through 2AR. Strong agonists for either receptor suppress signaling through the partner receptor and inverse agonists for either receptor potentiate the signaling through the partner receptor. To describe changes in the balance between Gi and Gq signaling induced by heteromeric assembly of the two receptors, we introduced a metric called the balance index (BI). Importantly, we demonstrated that the BI can predict the anti- or pro-psychotic activities of drugs targeting $mGlu_2R$ and 2AR. Drugs with the most effective antipsychotic properties, regardless of which receptor they target, show the highest BI values, whereas drugs with the most effective pro-psychotic properties show the lowest BI values.

The physiological relevance of cross-signaling between $mGlu_2R$ and 2AR was challenged in a concurrent publication by Delille and colleagues [6], and in a subsequent review by the same authors [7]. These authors reported that even though co-expression of the two receptors in HEK293 cells resulted in heteromeric complexes, as expected based on previous reports [13,32], no significant effects on either Gi or Gq signaling in response to 2AR or $mGlu_2R$ agonists, antagonists and positive allosteric modulators (PAMs) could be observed. Based on their results these authors argued against the relevance of cross-signaling between the two receptors for mammalian cells. In the present study we have addressed this controversy by using a system of HEK293 cells stably expressing various levels of the two receptors in the background of the GIRK1/4 channel that served as a reporter for both Gi and Gq signaling. Cross-signaling between $mGlu_2R$ and 2AR was investigated by co-administration of natural agonists to either receptor with inverse agonists of the partner receptor. Here we report that cross-signaling between the two receptors does exist in mammalian cells, however mere co-expression of the two receptors is not enough to guarantee cross-signaling. Only a fraction of our clones showed positive crosstalk (i.e. potentiation of the signaling of one receptor by inverse agonists targeting the partner receptor) as assayed by calcium imaging. Patch clamping and use of potentiometric dyes further confirmed these results in representative crosstalk positive and negative clones (the later defined as clones where inverse agonists for either receptor did not potentiate the signaling of the partner receptor). In accordance to our observations from *Xenopus* oocytes [11], appropriate ratios of the two receptors appear to be necessary for functional crosstalk. In our mammalian cell system, functional crosstalk correlated with increased colocalization of the two receptors at the cell surface and higher ratios of normalized $mGlu_2R$/2AR surface expression. Importantly, a combination of ligands targeting both receptors was able to elicit functional crosstalk in crosstalk-negative clones, indicating that even crosstalk-negative heterocomplexes can show cross signaling under the appropriate pharmacological treatment. These results further establish the functional significance of the heteromeric $mGlu_2R$/2AR complex and point to the gaps in our knowledge on what controls subunit stoichiometry and trafficking to the plasma membrane in crosstalk positive complexes in mammalian cells.

Methods

Constructs

The human GIRK1 and GIRK4 subunits of the atrial K^+ channel were sub-cloned within the multiple cloning sites MCS1 and MCS2, respectively, of the bidirectional expression vector pBI-CMV1 (Clontech Laboratories, Inc., Catalog # 631630). N-terminally c-Myc-tagged wild-type human 5-HT_{2A} (Myc-2AR) and N-terminally HA-tagged human $mGlu_2R$ (HA-$mGlu_2R$) have been previously described [13]. For antibiotic selection purposes, the above constructs were sub-cloned in the pcDNA3.1/hygro and pcDNA3.1/neo vectors, respectively. All constructs were confirmed by DNA sequencing. Constructs used in transient transfection controls for the binding assays: The N-terminally c-Myc-tagged form of the wild-type human 5-HT_{2A} and the N-terminally hemagglutinin (HA)-tagged form of wild-type $mGlu_2$, as well as substitution of residues Ala-$677^{4.40}$, Ala-$681^{4.44}$ and $Ala685^{4.48}$ in $mGlu_2R$ for $Ser686^{4.40}$, $Phe690^{4.44}$ and $Gly\text{-}694^{4.48}$ in $mGlu_3R$ (HA-$mGlu_2\Delta TM4N$) have been described previously [29]. Superscripts in this form indicate Ballesteros-Weinstein numbering for conserved GPCR residues [29]. It has also been shown that the $mGlu_2/mGlu_3$ chimeric construct does not form a heteromeric complex with 2AR [29].

Cells and transfections

HEK293 cells were maintained in Dulbecco's modified Eagle's medium (DMEM, Invitrogen, Carlsbad, CA) supplemented with 10% (v/v) fetal bovine serum at 37°C in a 5% CO_2 humidified atmosphere. Transfections were performed using Lipofectamine 2000 reagent (Invitrogen), according to manufacturer's instructions. For selection of the stably transfected GIRK clones, the pPUR selection vector (Clontech Laboratories, Inc., Catalog # 631601) was co-transfected with the pBI-CMV1-GIRK1-GIRK4 construct in 1:20 ratio and stable clones of HEK-GIRK cells were selected, and maintained thereafter, in puromycin-containing medium (500 ng puromycin/ml). For selection and maintenance of HEK-GIRK-$mGlu_2R$ clones, G418 (500 μg/ml) was included in the above medium, whereas HEK-GIRK-$mGlu_2R$-2AR clones were selected and maintained in the presence of the above antibiotics plus hygromycin (200 μg/ml).

Western blotting

Cell lysates were prepared in RIPA buffer (Santa Cruz Biotechnology, Santa Cruz, CA), containing Protease inhibitors (Roche Diagnostics, Basel, Switzerland). Equal amounts of protein were resolved by SDS-polyacrylamide gel electrophoresis and analyzed by immunoblotting. GIRK expression was detected with the anti GIRK1 polyclonal antibody H-145 (Santa Cruz Biotechnology, Santa Cruz, CA). The anti N-cadherin mouse monoclonal antibody (BD Transduction Laboratories, Franklin Lakes, NJ) was used to probe for N-cadherin, as an internal control. Expression of HA-tagged $mGlu_2R$ was detected by the rat anti-HA antibody 3F10 (Boehringer Mannheim, Mannheim, Germany).

Measurements of Intracellular Ca^{2+}

Cells were switched to serum-free medium for about 3–4 hours, before being loaded with 5 μm Fura2-AM (Molecular Probes, OR) in Imaging Solution (125 mM NaCl, 5 mM KCl, 2

mM $CaCl_2$, 1 mM $MgSO_4$, 6 mM glucose, and 25 mM Hepes/Tris, pH 7.4). Following incubation for 30 min at 37°C, cells were washed with imaging solution and kept at room temperature for about 15 min before being placed on the stage of an epifluorescence microscope, coupled to an automatic perfusion system and controlled by the Live Acquisition Software from Till Photonics, see [33] for details. The Fura-2 signal was acquired at 510 nm by switching the excitation wavelength between 340 nm and 380 nm. Intracellular calcium concentration was expressed as a 340/380 nm ratio and values were normalized to the basal 340/380 nm ratio level before perfusion of the drug. For the experiments presented in Figure 2, responses of each cell to either 5-HT or 5-HT + LY34 were further normalized to the mean 5-HT responses in cells from the same clone in the same experiment. Results were expressed as mean ± SEM. Statistical significance was determined by two tail Student's t test.

ImageStream and Immunofluorescence

Imaging flow cytometry was used to measure the $mGlu_2R$ and 2AR surface expression as well as colocalization of these receptors at a single cell level. HEK293 clones stably expressing $mGlu_2R$-HA or 2AR-c-Myc were fixed with paraformaldehyde (1.6%, 10 min at room temperature). Cells were not permeabilized to ensure only surface staining of the receptors. To avoid possible effects of the trypsin and/or EDTA on distribution of the receptor, cells were re-suspended mechanically. Our group has successfully applied this technique to assess HEK293 by regular flow cytometry [27]. Cells were then stained with an anti-HA mouse IgG1 monoclonal antibody conjugated with Alexa Fluor 488 (Cell Signaling, catalog # 2350S) together with an anti-c-Myc mouse IgG1 monoclonal antibody conjugated with Alexa Fluor 647 (Cell Signaling, catalog # 2233S) (1:25 dilution for 1 hour at room temperature). Controls were performed by staining a subset of the sample with the corresponding isotype antibodies, one conjugated to Alexa Fluor 488 (Cell Signaling, catalog #4878) together with one conjugated to Alexa Fluor 647 (Cell Signaling, catalog #4843). Following staining, images of each cell were acquired at a magnification of 60× on an ImageStream flow cytometer (Amnis) and analyzed with the IDEAS analysis software. Single-color controls were used for the creation of a compensation matrix that was applied to all files to correct for spectral crosstalk.

In surface receptor expression measurements calibration beads (Spherotech catalog # RCP-30–5A) were used to control for changes in the laser output power and image acquisition among different experiments. We further normalized the expression measurement to the size of each cell to obtain surface protein expression as densities.

For co-localization measurements positive cutoff values were calculated on the basis of the background 'bright detail similarity' (BDS) of $mGlu_2R$-HA and 2AR-c-Myc and an irrelevant signal (bright field) (see Fig. 3B). The BDS feature of IDEAS was then used for measurement of the spatial correlation between the fluorescent signal emanating from Alexa Fluor 488–labeled HA and that of Alexa Fluor 647-labeled 2AR-c-Myc. BDS is the log-transformed Pearson's correlation coefficient of the localized bright spots with a radius of three pixels or less within the masked area in the two input images.

$$\text{BDS score} = \ln\left[\frac{(1+\rho)}{(1-\rho)}\right]$$

The higher the BDS score, the higher the level of co-localization. BDS scores of >1.5 were considered co-localized. This threshold for the BDS score was obtained by applying the similarity image analysis algorithm first to a negative set (bright-field image). A threshold of 1.5 is consistent with previous similar studies [20,31] and indicative of good performance of the image analysis algorithm.

Confocal Microscopy

Cells were plated in coverslips and were allowed to attach overnight. Cells were then fixed and stained with an anti-HA mouse IgG1 monoclonal antibody conjugated with Alexa Fluor 488 (Cell Signaling, catalog # 2350S) together with an anti-c-Myc mouse IgG1 monoclonal antibody conjugated with Alexa Fluor 647 (Cell Signaling, catalog # 2233S) (1:25 dilution for 1 hour at room temperature). Controls were performed by staining coverslips with the corresponding isotype antibodies, one conjugated to Alexa Fluor 488 (Cell Signaling, catalog #4878) together with another conjugated to Alexa Fluor 647 (Cell Signaling, catalog #4843). Additional controls with untransfected HEK293 to test selectivity of antibodies were also performed. Following staining, coverslips were mounted and imaged with a Zeiss LSM880 laser confocal microscope using a 40× oil-immersion objective. Colocalization signal was determined performing a pixel-by-pixel comparison of the 2AR-c-Myc and the $mGlu_2R$-HA images after background subtraction based on isotype controls. Microscopy was performed at the Microscopy CORE at the Icahn School of Medicine at Mount Sinai. Image analysis was performed with Matlab (http://www.mathworks.com).

Gene Expression Measurements

Messenger RNA expression was quantified using quantitative RT-PCR. cDNA was synthesized from total RNA using AffinityScript MultiTemp RT (Agilent, Santa Clara CA) with an oligo(dT)18 primer. Realtime PCR was performed using PlatinumTaq DNA polymerase (Invitrogen, Carlsbad CA) and SYBR-green (Invitrogen, Carlsbad CA) on an ABI7900HT thermal cycler (Applied Biosystems, Foster City CA). A robust global normalization algorithm, using expression levels of the housekeeping genes ribosomal protein S11 (*rps11*), β-actin (*actb*), and α-tubulin (*tuba*), was used for all experiments, as described elsewhere [3]. In brief, all crossing threshold (Ct) values were first adjusted by median difference of all samples from *actb*. Each individual sample was then further corrected by the median Ct value of the three corrected housekeeping controls for that sample. Finally, nominal copy numbers were calculated by assuming 2500 molecules of actb mRNA per cell, and an amplification efficiency of 93% using the difference in Ct value (ΔCt method). PCR primer sequences for $mGlu_2R$ used are GCTACGCCTCTACCAGTGCCAA for the sense and ATGCCTGTCTCGCCATAGTCG for the antisense. PCR primer sequences for 2AR used are CCACAGCCGCTTCAACTCC for the sense and TCGAATCGTCCTGTAGCCCAA for the antisense.

Radioligand binding assays

Radioligand binding assays in total membrane preparations were performed as described previously [29] with minor modifications. Briefly, cell pellets (transfected HEK293 cells or clones) were homogenized using a Teflon-glass grinder (10 up-and-down strokes at 1500 rpm) in 1 ml of binding buffer (see below), supplemented with 0.25 M sucrose. The crude homogenate was centrifuged at 1000 × g for 5 min at 4°C, and the supernatant was re-centrifuged at 40,000 × g for 15 min at 4°C. The resultant pellet (P_2 fraction containing both plasma membranes and endosomes) was washed twice in homogenization buffer and recentrifuged in similar conditions. Aliquots were stored at −80°C until the assay was carried out. Protein concentration was determined using the Bio-Rad protein assay.

[^{3}H]Ketanserin binding was performed as previously reported with minor modifications [29]. [^{3}H]Ketanserin was purchased from PerkinElmer. Binding saturation curves were performed using 9 concentrations of [^{3}H]ketanserin (0.0625–10.0 nM). Competition curves were carried out by incubating DOI (10^{-10} – 10^{-4} M; 14 concentrations) in binding buffer containing 2 nM [^{3}H]ketanserin. Non-specific binding was determined in the presence of 10 μM methysergide (Tocris).

[^{3}H]LY341495 (or LY34) binding was performed as previously reported with minor modifications [29]. [^{3}H]LY341495 was purchased from American Radiolabeled Chemicals, Inc. Binding saturation curves were performed using 11 concentrations of [^{3}H]LY341495 (0.0625–30.0 nM). Non-specific binding was determined in the presence of 1 mM L-glutamic acid (Sigma).

Radioligand binding data were analyzed using a non-linear curve fitting software (GraphPad Prism). An extra-sum-of-squares (F-test) was used to determine statistical difference for simultaneous analysis of saturation and displacement curves.

Whole-cell patch-clamp recordings

Whole-cell patch-clamp current recordings were performed with either Patch Clamp L/M-EPC7 or Axopatch 200A and 200B amplifiers and Axon 8.1 software (Axon Instruments, Union City, CA). Cells were trypsinized, resuspended in DMEM medium and placed in the incubator for at least 3–4 hours for recovery. After recovery, cells were placed on poly-D-lysine coverslips, left to attach for ~15 minutes, and transferred to the chamber of the patch-clamp setup with external solution containing in mM: 140 Potassium gluconate, 2 $CaCl_2$, 5 EGTA/K, 10 Glucose, 10 HEPES-K and 1 $MgCl_2$. The composition of the internal solution was in mM: 140 Potassium gluconate, 2 $CaCl_2$, 5 EGTA/K, 10 Glucose, 10 HEPES-K, 0.3 $MgCl_2$, 2 NaATP and 0.01 GTP. Osmolarity in both solutions was 340 mOsm and pH was 7.4. Upon formation of the whole-cell configuration, a voltage ramp from −100mV to +100mV was applied and data were collected. At the end of the recordings, 4 mM $BaCl_2$ was applied to block potassium currents. The first few data points of the current versus time plot at −100 mV were averaged to obtain basal current. Similarly, agonist-induced currents were calculated by averaging several current values at the peak of the effect. Values were divided by the membrane capacitance (pF) to normalize for the size of each cell. For the experiments shown in Figure 6A, Gq activity was measured as GIRK current inhibition. Gq-

induced changes were subtracted from basal and the difference was divided by the basal currents. For the experiments shown in Figures 6B, C, Gi activity was measured as GIRK current activation. Basal levels were subtracted from agonist-induced values and the difference was divided by the basal currents.

HLB 021–152 epifluorescence assay

A day before the assay the cells were plated in black-walled, clear-bottomed 96-well microplates (Greiner Bio-One GmbH) and incubated overnight in serum-containing medium. The following day cells were switched to serum-free medium for about 2–3 hours before switching again to low-K^+ assay solution (125 mM NaCl, 2 mM KCl, 2 mM $CaCl_2$, 1 mM $MgSO_4$, 6 mM glucose, and 25 mM HEPES/Tris, pH 7.4) containing HLB021–152 (5μM; AnaSpec). Dye-loaded cells were incubated at 37 °C for 45 min and kept at room temperature for about 15 min before being transferred to an epifluorescence microscope, coupled to an automatic perfusion system. Cells were excited at 530 nm and fluorescence was recorded at the 590/40 nm band at 2 sec intervals. Baselines were recorded for 60 sec by constant perfusion of Low-K^+ assay solution containing HLB 021–152 before perfusion of the drugs, again in dye- containing Low-K^+ assay solution. Fluorescent traces obtained for each cell were analyzed as follows; Fluorescent signals for each time point were divided by the average signal of the last 20 sec of the baseline to obtain F/F0. Drug-induced changes in fluorescence were calculated by averaging 5–6 values of the F/F0 trace at the peak of the effect. Data were expressed as the percentage of change in channel activity (i.e. the percentage of decrease in fluorescence in each cell compared to its baseline).

Fluorescent imaging plate reader FLIPR membrane potential assay

Two days before the assay the cells were plated in black-walled, clear-bottomed 96-well microplates (Greiner Bio-One GmbH) so as to be approximately 90% confluent on the day of the assay. Cells were switched to serum-free medium for about 2–3 hours, following which an equal volume of the dye (FLIPR Membrane Potential dye (blue) from Molecular Devices, Sunnyvale, CA), reconstituted in low-K^+ assay solution, was added. Dye-loaded cells were incubated at 37 °C for 45 min and transferred to an automated liquid handling microplate reader (FlexStation 3 Molecular Devices). Fluorescence was measured at 565 nm with an excitation wavelength of 530 nm and cutoff at 550 nm. Data points were collected at 2 sec intervals. Basal fluorescence was recorded for 60sec before addition of the drugs in dye- containing assay solution. Control wells received only vehicle. Fluorescent signals for each time point were divided by the average signal of the last 20 sec of the baseline to obtain F/F0. F/F0 values from 6–8 control wells were averaged and the average control F/F0 values were subtracted from F/F0 values in each of the drug-treated wells from the same plate in order to obtain normalized traces. Drug-induced changes in fluorescence were calculated by averaging 5–6 values of the normalized trace at the peak of the effect.

Results

Generation of stable cell lines expressing 2AR and $mGlu_2R$ in the background of GIRK1/4 channel (HEK/GIRK/$mGlu_2R$/2AR clones)

To investigate whether $mGlu_2R$ and 2AR can cross-signal in HEK293 cells, we proceeded to generate stable cell lines expressing the two receptors in the background of the Kir3.1/3.4 (or GIRK1/GIRK4) inwardly rectifying channel, which serves as a reliable reporter for both Gq and Gi signaling [14,23]. HEK293 cells were transfected with the bidirectional expression vector pBI-CMV1, carrying the GIRK1 and GIRK4 subunits of the channel and antibiotic resistant clones were screened by Western blotting for expression of GIRK1 (Fig. 1a, lower panel). Levels of endogenously expressed N-cadherin served as internal loading controls (Fig. 1a, upper panel). In order to select the appropriate clone to then add the receptors to, we searched for clones expressing suitable levels of functional heteromeric GIRK1/4 channel. Several GIRK1-positive clones were subjected to whole-cell patch-clamp recordings to monitor responses to the guanosine triphosphate analog GTPγS, which is known to stimulate receptor-independent activation of barium-sensitive GIRK currents [4]. Indeed, inclusion of GTPγS in the patch pipette stimulated basal currents by several fold in most of the clones tested, an effect blocked by $BaCl_2$ added to the bath solution. Figure 1b shows a summary of data obtained from clone 31, the clone we eventually chose to express the GPCRs (see Online Resource 1, Fig. S1a) for a representative trace. We next proceeded to transfect an HA-tagged $mGlu_2R$ in the GIRK1/4 expressing HEK293 cell clone 31 (HEK/GIRK 31). Antibiotic-resistant clones were first screened for expression of $mGlu_2R$ by Western blotting with anti-HA antibodies (Fig. 1c). In order to confirm functional coupling of the receptor to the channel, clones positive for $mGlu_2R$ expression were subjected to whole-cell patch-clamp recordings and tested for Glutamate- (Glu-) induced currents. Indeed, in several clones, application of Glu induced a significant increase in the activity of the channel, which was blocked by $BaCl_2$ (see Online Resource 1, Fig S1b for a representative trace). The HEK/GIRK/$mGlu_2R$ clone 59 (summary of responses to 100 μM of Glu are shown in Fig. 1d) was selected for stable transfection of a c-Myc-tagged 5-$HT_{2A}R$ (or 2AR). In order to efficiently screen antibiotic resistant clones for 2AR expression, we relied on the transient increase of intracellular calcium due to IP3-mediated Ca^{2+} release from the endoplasmic reticulum following stimulation of Gq signaling. The ratiometric calcium indicator Fura2-AM was used to detect 5-HT-induced elevation of intracellular calcium in the 2AR expressing clones by epifluorecence microscopy. Upon serotonin (5-HT) application, most clones showed a transient 5-HT-dependent increase in the FURA-2 emission ratio (2AR-positive clones, see Fig. 1e and Online Resource 2, Video 1), whereas several clones were insensitive to 5-HT (2AR-negative clones, see Fig. 1f and Online Resource 3, Video 3), presumably indicating that they had not integrated 2AR in their genome. Many of the stable cell lines contained the desired GPCRs and the channel reporter, but the question remained of whether the presence of these three components was sufficient to give crosstalk. Characterizing a number of stable HEK/GIRK/$mGlu_2R$/2AR cell lines with different levels of expression of $mGlu_2R$ and 2AR provided us with the opportunity to identify the characteristics required for cross-signaling between heteromers of these two receptors in mammalian cells.

Cross-signaling between $mGlu_2R$ and 2AR in HEK/GIRK/$mGlu_2R$/2AR clones, demonstrated by calcium imaging

We first studied crosstalk from the $mGlu_2R$ to the 2AR side of the heteromer displayed by these clones. We have previously shown that upon co-expression of $mGlu_2R$ and 2AR in the *Xenopus* oocyte system, the $mGlu_2R$ inverse agonist LY341495 (or LY34) cross-signals and potentiates the 5-HT-elicited Gq signaling [11]. To examine whether such a crosstalk between the two receptors existed in our stably transfected HEK/GIRK/$mGlu_2R$/2AR cell system, we used calcium imaging to compare Gq signaling-induced calcium release in response to 5-HT, in the presence and absence of LY34. Preliminary experiments confirmed that LY34 alone was not able to elicit any calcium responses. Randomly selected 2AR-positive clones were exposed to 5-HT, or 5-HT together with LY34, and the calcium signal was measured by the ratiometric calcium indicator Fura-2. Multiple independent experiments confirmed that cross-signaling between the two receptors, as manifested by potentiation of the serotonin-induced signal, is a characteristic of a fraction of the 2AR-positive clones. However, stable transfection produced a variety of clones with different phenotypes. While about 25–30% of the clones showed consistent potentiation of the 5-HT-induced signal by LY34 (crosstalk positive), most of the 2AR-positive clones failed to show LY34-dependent potentiation of the 5-HT-induced signal (crosstalk negative). Figures 2a and 2b show a summary of LY34-potentiated fluorescence data obtained from different clones, with either saturating (Fig. 2a) or sub-saturating (Fig. 2b) concentrations of 5-HT. It should be noted than even under saturating concentrations of serotonin we never observed saturation of the Fura-2 signal; a) application of the Ca^{2+} ionophore 4Br-A23187 under identical conditions yielded much larger Ca^{2+}signals and b) LY34 had quantitatively similar effects under either a saturating or sub-saturating concentration of 5-HT in two clones used in both sets of experiments (see clones 45 and 106 in Figures 2a and 2b).

Among the clones tested, two clones displayed unexpected responses: One of them, clone 3, showed a consistent and highly significant suppression of the serotonin signal (Online Resource 4, Fig. S2a). This behavior signifies a unique phenotype, which is neither crosstalk positive (no potentiation of the 5-HT signal by LY34), nor crosstalk negative (since a drug targeting one receptor did induce highly reproducible changes in the signaling of the partner receptor). The nature of this unique inverse cross-signaling is unclear. Another clone, 92, unlike any other clone, displayed inconsistent responses appearing as crosstalk positive in some of the calcium imaging experiments but as crosstalk negative in others (see Onine Resource 4, Fig. S2b). However, despite its inconsistent behavior in the LY34 potentiation of the 5-HT-induced calcium imaging assay, this clone showed a consistent crosstalk-positive phenotype in all other assays tested (presented in the relevant sections of the Results).We also expand on the unexpected responses of these two clones in the Discussion.

Cells from crosstalk-positive clones show a higher degree of colocalized signal for $mGlu_2R$ and 2AR

Based on the reasonable assumption that crosstalk-positive clones will express greater amounts of the $mGlu_2R$/2AR heteromers in the membrane, we hypothesized that crosstalk-positive clones would exhibit a greater extent of colocalization of the $mGlu_2R$ and 2AR in the membrane. Imaging flow cytometry has successfully been used to quantify

colocalization of proteins [2,20,27,31]. We chose to use imaging flow cytometry since it provides a unique tool to quantify colocalization in a large number of cells and is perfectly adapted to screen multiple clones. We then validated these results with confocal microscopy in a crosstalk-positive clone (clone 80) and a crosstalk-negative clone (clone 45).

We first mechanically (without trypsin or EDTA) resuspended HEK/GIRK/mGlu_2R/2AR cells from different clones to avoid disruption of receptor expression. Samples were then fixed and stained with antibodies against the extracellular HA and c-Myc tags included in the stably-transfected mGlu_2R and 2AR constructs respectively, conjugated to two non-overlapping fluorophores, Alexa Fluor 488 and Alexa Fluor 647. For each cell (10,000 cells/sample), bright field, mGlu_2R-HA staining, and 2AR-c-Myc staining images were obtained using Image Flow (Fig. 3a). In order to ensure surface staining exclusively, cells were not permeabilized. Thus, despite these images being epifluoresnce images, any signal captured in the image is strictly on the surface. We quantified colocalization in each cell by comparing the bright detail similarity (BDS) between the signals associated with each receptor (see Methods). We obtained the threshold for highly-colocalized signals in the analysis of BDS=1.5 by applying the similarity image analysis algorithm first to a negative set of images (bright-field images). The threshold of 1.5 (Fig 3b) is consistent with previous similar studies [31,20] and was indicative of good performance of the image analysis algorithm.

Consistent with our hypothesis, quantification of the colocalization extent of mGlu_2R and 2AR signals in the membrane of cells from different clones revealed a significant increase in the percentage of cells with highly-colocalized mGlu_2R and 2AR signals (colocalized cells) in crosstalk-positive clones, compared to crosstalk-negative clones (Figs. 3b, 3c). Clone 3, which showed inverse cross-signaling in the calcium imaging experiments (see Onine Resource 4, Fig. S2a) showed low levels of colocalization, comparable to the consistently crosstalk-negative clone 45 (see Online Resource 4, Fig. S2c). In contrast, clone 92, which showed inconsistent responses in the calcium imaging experiments (see Online Resource 4, Fig. S2b), showed a much higher percentage of colocalization, comparable to those observed in the crosstalk-positive clones (see Online Resource 4, Fig. S2c and also Fig. 3c for comparison).

To validate our results we obtained images of the cell-membrane distribution of mGlu_2R and 2AR in cells from clone 45 (crosstalk-negative) and clone 80 (crosstalk-positive), using confocal laser microscopy. We evaluated the extent of the colocalization of the mGlu_2R and 2AR by calculating the BDS of their respective confocal microscopy images (Fig. 3d). BDS control measurements with Bright Field images yielded an average score of 0.093 (the BDS threshold of 1.5 is only applicable to single cells). Controls in unstransfected HEK293 cells and with isotype staining were also performed. Our results indicated a higher extent of colocalization for the crosstalk-positive clone supporting our imaging flow cytometry results

Crosstalk-positive and crosstalk-negative clones are differentiated based on the relative surface expression of the receptors, each normalized to its own mRNA level

In an effort to further understand the cross-signaling responses of individual clones, we proceeded to characterize differences between crosstalk-*positive* and crosstalk-negative clones in terms of protein and gene expression.

We first measured by immunofluorescence and flow cytometry the ratios of surface (non-permeabilized cells) protein expression of $mGlu_2R$ and 2AR in different clones, utilizing the fluorophore-conjugated anti-HA and anti-c-Myc antibodies described above. We observed that the $mGlu_2R$ and 2AR surface expression levels did not explain the difference between crosstalk-positive and crosstalk-negative clones (Fig. 4a) and neither did the ratio between the two levels of receptor surface expression (Fig. 4b).

We then used the real-time polymerase chain reaction (RT-PCR) to measure the level of $mGlu_2R$ (*GRM2*) and 2AR (*HTR2A*) gene expression. Stably transfected cells, showed high degree of variability in $mGlu_2R$/2AR mRNA ratios, which ranged from 1:1 to more than 4:1 (Fig. 4c). Notably, crosstalk-positive clones were characterized by ratios around 1:1 (i.e. closer to 0.5 seen in the positive crosstalk experiments in *Xenopus* oocytes by Fribourg at al [11], whereas crosstalk-negative clones were largely characterized by higher $mGlu_2R$/2AR mRNA ratios. A few exceptions however, e.g. clone 88 shown in Fig. 4c, suggested that mRNA ratios of our stably transfected receptor clones may not be sufficient to differentiate crosstalk-positive from crosstalk-negative clones.

Interestingly, and in line with our previous results in oocytes [11], the expression levels for each gene did not correlate with the amounts of surface protein expressed (compare Fig. 4b and Fig. 4c). Guided by the existing literature that indicates differences in translation and trafficking of heteromers vs. homomers [16,5,26], we explored whether normalizing each surface receptor protein to its available mRNA could differentiate crosstalk-positive from negative clones. Indeed, the ratio $mGlu_2R$ and 2AR surface protein expression (immunofluorescence measurement), each expressed per unit of its own mRNA (RT-PCR measurement), revealed statistically significant differences that allowed us to reliably differentiate functionally crosstalk-positive from crosstalk-negative clones (Fig. 4d). Similarly to what we observed in the colocalization experiments, clones 3 and 92, characterized by their unexpected behavior in calcium imaging experiments, were among the crosstalk-negative and crosstalk-positive groups, respectively (see Online Resource 4, Fig. S2d).

Plotting the normalized $mGlu_2R$ surface protein (surf. protein/mRNA) against the normalized 2AR surface protein for each clone revealed a clear segregation of crosstalk positive clones to a different area than the one corresponding to the negative ones (Online Resource 4, Fig. S2e, grey and white areas, respectively). Remarkably, the “peculiar” clones 3 and 92 appear very close to the borderline dividing the crosstalk-positive and crosstalk-negative regions, which presumably explains their unexpected behavior.

Ligand binding interactions in a representative pair of crosstalk-positive and crosstalk-negative clones

As, mentioned above, ratios of $mGlu_2R$/2AR mRNA expression levels in different clones did not correlate with the corresponding surface protein expression ratios (compare Fig. 4b and Fig. 4c), similar to results in *Xenopus* oocytes where for a given $mGlu_2R$ mRNA level, the amount of the injected RNA for 2AR accounted for levels of total, but not of surface receptor protein [11]. Radioligand binding assays in crude membrane preparations offer a sensitive measure of the relative densities of the total levels of a transmembrane receptor in two samples. To determine the total densities of $mGlu_2R$ and 2AR in a representative pair of crosstalk positive and negative clones, we carried out radioligand binding assays in total membrane preparations (i.e., P_2 fraction containing plasma membranes and intracellular membrane compartments) from clone 80 (crosstalk positive) and clone 45 (crosstalk negative). Binding assays saturation curves with the $mGlu_{2/3}R$ receptor antagonist [^{3}H]LY341495 indicated higher density of $mGlu_2Rs$ in clone 45 as compared to clone 80 (Fig. 5a and Table 1), whereas binding assays saturation curves 2AR receptor antagonist [^{3}H]ketanserin indicated a higher density of 2ARs in clone 80 as compared to clone 45 (Fig. 5b and Table 1). Thus, in line with the observation that the crosstalk positive phenotype is largely associated with lower $mGlu_2R$/2AR mRNA ratios, the crosstalk-positive clone 80 displayed both lower density of total $mGlu_2Rs$ and higher density of total 2ARs, compared to the crosstalk-negative clone 45, resulting in a lower ratio of $mGlu_2R$/2AR total receptor density, as determined by the ratio of [^{3}H]LY341495 / [^{3}H]ketanserin binding sites (Fig. 5c).

When a non-radioactive agonist ligand is used to displace an antagonist radioligand, it will first bind receptor–G-protein complexes and then, at higher concentrations, it will compete for the uncoupled receptors. This results in the well-characterized biphasic displacement curves of radiolabeled antagonists seen with agonists [13]. We have previously demonstrated that the biphasic displacement curve of [^{3}H]ketanserin by the 2AR agonist DOI becomes monophasic in cells co-expressing 2AR and $mGlu_2R$ [29]. We also reported that this allosteric crosstalk between 2AR and $mGlu_2R$ requires close sub-cellular proximity as it is absent in cells co-expressing 2AR and the $mGlu_2R/mGlu_3R$ chimeric construct that does not form the 2AR-$mGlu_2R$ heteromeric complex ($mGlu_2R\Delta TM4N$) [29]. Similar findings were observed in this study (Figs. 5d and 5e, and Table 1). Displacement of [^{3}H]ketanserin binding by DOI became monophasic in crude membrane preparations of clone 80 (Fig. 5e and Table 1), whereas competition binding experiments of [^{3}H]ketanserin by DOI in clone 45 were still best described by a two-site model (Fig. 5e and Table 1), as shown previously with the 2AR alone (Fig. 5e and Table 1). However, the fraction of high-affinity sites for DOI in clone 45 was decreased compared to that observed in cells expressing 2AR alone (Fig. 5e and Table 1), presumably indicating a low level of crosstalk between $mGlu_2R$ and 2AR in this clone.

Cross-signaling between $mGlu_2R$ and 2AR in HEK/GIRK/$mGlu_2R$/2AR clones using an electrophysiological assay

In the *Xenopus* oocyte system, cross-signaling between $mGlu_2R$ and 2AR results in potentiation of the signaling of either receptor in response to its endogenous ligand by inverse agonists of the partner receptor [11]. To further differentiate between a crosstalk-

positive and a crosstalk-negative stable HEK293 clone, we performed whole-cell patch-clamp recordings of the activity of the GIRK channel in response to the combination of the endogenous ligand together with an inverse agonist targeting each of the two receptors. GIRK channels are known to be directly activated by the Gβγ subunits of Gi/o proteins [24]. GIRK channel activation has been extensively used as a measure of Gi signaling [14,15,34]. In contrast, the activity of GIRK channels is inhibited by Gq/11 signaling via hydrolysis of phosphatidylinositol-4,5-biphosphate (PIP_2), a membrane phospholipid critical for the maintenance of channel activity [25]. Upon Gq/11 activation, phospholipase C (PLC) hydrolyzes PIP_2 into diacylglycerol (DAG) and inositol triphosphate (IP_3). PLC-mediated PIP_2 depletion results in desensitization of GIRK currents [23] and the level of current inhibition can be used as a measure of the elicited Gq activity.

First, the $mGlu_2R$ inverse agonist LY34 potentiated the 5-HT-induced Gq activity of our crosstalk-positive (clone 80) but not that of a crosstalk-negative clone (clone 45) (Fig. 6a, see Online Resource 5, Fig. S3a for representative traces), consistent with our Ca^{2+} imaging data (Fig. 2b). We next tested whether the inverse agonist of 2AR Paliperidone could cross-signal and potentiate the $mGlu_2R$-mediated response to glutamate (Glu). The same two clones used for the experiments of Figure 6a were subjected to whole-cell recordings of GIRK channel activity stimulated by sequential application of Glu and Glu together with Paliperidone. Paliperidone potentiated Glu-induced GIRK currents for clone 80 but not for clone 45 (Fig. 6b, see Online Resource 5, Fig. S3b for representative traces).

A combination of an $mGlu_2R$ strong agonist together with a 2AR inverse agonist has previously been shown as necessary in order to elicit cross-signaling in cases of suboptimal expression ratios of the two receptors [11]. We asked whether a combination of the 2AR inverse agonist Paliperidone with the $mGlu_2R$ strong agonist LY37379268 (or LY37) would elicit cross-signaling in the crosstalk negative clone 45 but not further cross-signaling in the crosstalk positive clone 80. Sequential application of LY37 and LY37 plus Paliperidone was used to stimulate GIRK channel activity. As expected, LY37 was more efficacious than Glu in stimulating GIRK currents (note the scale difference in Fig. 6b versus 6c). Application of Paliperidone plus LY37 promoted a significant increase in LY37-stimulated GIRK channel activity in clone 45 but not the crosstalk positive clone 80 (Fig. 6c, see Online Resource 5, Fig. S3c for representative traces), which, in agreement with our binding data from this clone indicating some low level of cross signaling, suggests that this clone retains the ability to show cross signaling in response to the combination of the $mGlu_2R$ strong agonist with the 2AR inverse agonist.

In summary, the above data strongly support cross-signaling between the two receptors, as manifested by potentiation of the signaling of either receptor by inverse agonists of the partner receptor, in crosstalk positive clones. Moreover, our data suggest that by acting on both receptors simultaneously with the appropriate combination of drugs, we can improve weak cross-signaling between the two receptors due to sub-optimal expression ratios and rescue the crosstalk-negative phenotype, consistent with our prior results in the oocyte expression system [11].

Cross-signaling between $mGlu_2R$ and 2AR in HEK/GIRK/$mGlu_2R$/2AR clones, using fluorescence assays

We next proceeded to use fluorescent assays to test for cross-signaling of positive clones with the goal to efficiently test many cells simultaneously. Potentiometric probes offer an indirect method of detecting channel activity by measuring changes in membrane potential. The HLB 021–152 potentiometric dye has been successfully used to measure cyclic nucleotide gated ion channel activity in response to changes in cAMP concentration [37], or GIRK1/GIRK2 channel activity in response to muscarinic [40] or somatostatin [38,41] receptor activation. The negatively charged dye equilibrates across the plasma membrane of resting cells and fluoresces upon binding to proteins or lipids. Plasma membrane hyperpolarization triggered by K^+ channel opening decreases the levels of the cell-associated dye to the inner leaflet of the plasma membrane and results in a decrease in fluorescence.

We evaluated the suitability HLB 021–152 to report both Gi- and Gq-induced changes in GIRK channel activity in our system. We used epifluorescence microscopy coupled to an automatic perfusion system in order to measure changes in fluorescence at the single cell level. Figure 7a shows a representative summary of traces from the crosstalk-positive HEK/GIRK/$mGlu_2R$/2AR clone 106 Application of Glu promoted a decrease in fluorescence which was reversed by subsequent co-application of Glu together with the GIRK channel inhibitor Tertiapin Q (Trtn), indicating that the decrease in fluorescence was due to GIRK channel activation (Fig.7a, see also Online Resource 6, Video 3). To further confirm specificity of the responses, the parental clone HEK/GIRK 31, which expresses the channel but not the receptors, was subjected to the same protocol and such changes in fluorescence were not observed (Fig. 7a, ctrl 31, see also Online Resource 7, Video 4). Figure 7b shows a summary of the data presented as channel activity (See Online Resource 8, Figs. S4a and S4b for individual traces before averaging). Thus HLB 021–152 can reliably report Gi-dependent stimulation of GIRK channel activity upon agonist-dependent activation of $mGlu_2R$. We next asked whether HLB 021–152 would be a reliable reporter of GIRK channel activity regulated by switching between Gi and Gq signaling. HLB 021–152-loaded HEK/GIRK/$mGlu_2R$/2AR clones 80 and 106 and the control parental clone HEK/GIRK-31 were exposed to Glu to induce Gi signaling through $mGlu_2R$, followed by addition of 5-HT to induce Gq signaling through 2AR. As shown in Figure 7c (see also Online Resource 9, Video 5), Glu-induced changes in the HLB 021–152 fluorescent signal were reversed by subsequent addition of 5-HT (see Online Resource 10, Fig. 5 for individual traces before averaging). Figure 7d shows summary data from these two positive clones, expressed as channel activity. Our data indicate that HLB 021–152 serves as a reliable probe for changes in GIRK channel activity triggered by both Gi and Gq signaling. However the small fluorescence changes obtained with HLB 021–152 did not provide the appropriate dynamic range to accurately report signaling responses to a combination of drugs, particularly in view of the sensitivity of the dye to DMSO at concentrations as low as 0.5%, which complicated the use of compounds needing to be dissolved to DMSO (e.g. Paliperidone).

The FLIPR Membrane Potential dyes “Blue” and “Red” have been introduced as a generation of potentiometric probes with shorter response times, higher dynamic range and

less sensitivity to temperature changes. The FLIPR Blue dye has been successfully used to monitor GIRK channel activity in response to μ-opioid receptor activation in AtT-20 cells [22]. We tried both Blue and Red dyes in a high throughput setting, using an automated liquid handling microplate reader (FlexStation 3). Figure 8 shows data obtained using the Blue dye in this setup. As with the HLB 021–152 dye, application of Glu promoted a rapid decrease in fluorescence in cells from two crosstalk positive clones expressing the channel and the receptors (Figs. 8a and 8c), but not in control cells from the parental clone 31 expressing the channel but not the receptors (Figs. 8b and 8c). The effect of Glu was reversed by subsequent addition of 5-HT (See Figs. 8d, 8f), demonstrating the suitability of the dye to monitor both Gi- and Gq-dependent responses. Again no responses were recorded in the control clone 31 (Fig. 8e and 8f).

We next asked whether the FLIPR Blue dye would be a reliable reporter for cross-signaling responses similar to those recorded with whole-cell patch clamping (see Fig. 6b). Two of our crosstalk positive clones and the parental clone HEK/GIRK/$mGlu_2R$-59, which expresses the channel and $mGlu_2R$, but not 2AR, were used to determine whether the 2AR inverse agonist Paliperidone could cross-signal to potentiate $mGlu_2R$-dependent Gi signaling. Figure 8g shows sample traces from sequential application of Glu and Glu together with Paliperidone in dye-loaded cells from clone 80. Indeed co-application of Glu and Paliperidone promoted a significantly higher decrease in the FLIPR Blue fluorescence signal than Glu alone, indicating that the inverse agonist for 2AR cross-signaled to potentiate Gi signaling through the partner receptor $mGlu_2R$. Such responses to Paliperidone were not observed in cells from the control clone which does not express 2AR (Fig. 8h), confirming that Paliperidone acted through the $mGlu_2R$/2AR heteromer. Figure 8i summarizes the data from these experiments. Clone 92, appearing at the borderline between crosstalk-positive and crosstalk-negative clones (Online Resource 4, Fig. S2e), showed a crosstalk-positive phenotype in this assay (see Online Resource 4, Fig. S2f). It should be noted that although the FLIPR Blue potentiometric dye could provide a reliable probe not only for both Gi and Gq signaling but also for reporting cross-signaling between the two receptors, we found a highly variable sensitivity to DMSO among different batches of this dye.

In summary, our data from potentiometric dye probing suggest that both HLB 021–152 and FLIPR Blue potentiometric dyes provide reasonable probes for monitoring $mGlu_2R$- and 2AR- regulated GIRK channel activity and fully agree with our calcium imaging and whole-cell patch-clamp data showing cross signaling between $mGlu_2R$ and 2AR in representative clones of HEK293 cells expressing both receptors.

Discussion

In this study we stably expressed the $mGlu_2R$ and 2AR receptors along with a channel reporter (GIRK1/GIRK4) in HEK293 cells. Making single-cell epifluorescence Fura-2 measurements, we screened as crosstalk positive those clones that gave significantly higher 5-HT-induced Ca^{2+} responses in the presence of the inverse $mGlu_2R$ agonist LY34. Approximately 25–30% of the clonal cells we generated proved crosstalk positive. Such clones showed significantly higher cell surface colocalization of the two receptors than crosstalk negative ones, as assessed by imaging flow cytometry or confocal laser

microscopy. Moreover, when the cell surface $mGlu_2$/2A receptor ratio was normalized to each receptor's own mRNA, crosstalk-positive clones could be clearly differentiated from crosstalk-negative ones. Representative crosstalk-positive and negative clones were compared further in terms of their binding to radioactive $mGlu_2R$ and 2AR ligands, or the ability of a 2AR agonist to displace the radioactive 2AR inhibitor. Our binding results clearly differentiated the crosstalk-positive from negative clones, consistent with previously established positive and negative controls. We employed two additional functional assays using the channel reporter in these stably transfected cells to compare representative crosstalk-positive and negative clones. Whole-cell patch-clamp electrophysiological data were consistent with the Fura-2 fluorescence data in LY34 potentiation of 5-HT responses for a crosstalk-positive but not a negative clone. Similarly, the 2AR inverse agonist Paliperidone potentiated Glu responses for a crosstalk-positive but not a negative clone. Moreover, consistent with our previous data in *Xenopus* oocytes, combination of a 2AR inverse agonist with a strong $mGlu_2R$ agonist significantly enhanced cross signaling in a crosstalk negative rather than a positive HEK293 clone. In a second functional assay, we used potentiometric fluorescent dyes to report on channel activity as a result of Gi and Gq signaling activation in representative crosstalk positive and crosstalk negative clones. Using a FLEX station set-up, we measured signals from thousands of cells, and obtained significant potentiation of the Glu responses by Paliperidone in crosstalk-positive clones compared to negative controls. These results provide strong evidence that stably transfected mammalian cells can and do display cross-signaling through the $mGlu_2$ and 2A receptors.

The question then becomes what makes a clone crosstalk positive or negative as assayed by single ligands, even though it may be expressing both receptors? As was shown by Fribourg and colleagues in the *Xenopus* oocyte expression system [11] (also see [28]), the relative levels of $mGlu_2R$ and 2AR mRNA injected is a crucial factor of whether the formed heterocomplex would cross-signal or not in response to ligands targeting one or the other receptor. At the optimal $mGlu_2R$/2AR mRNA ratio, maximal cross-signaling correlated with the most efficient presentation of each receptor's protein at the cell surface. At sub-optimal $mGlu_2R$/2AR mRNA ratios, a condition associated with a dramatically reduced degree of cross-signaling, the ratio of $mGlu_2R$/2AR total receptor protein (although still following the ratio of injected RNAs) did no longer account for the ratio of receptor proteins at the cell surface, presumably indicating unfavorable changes in the trafficking and/or stability of the receptors at the cell surface. Although in a mammalian cell system the ratio of receptor mRNAs cannot be controlled as precisely as in the *Xenopus* oocyte system, our data indicate that similar regulatory mechanisms exist in mammalian cells. In the *Xenopus* oocyte system the optimal $mGlu_2R$/2AR mRNA ratio was 1:2. In the HEK/GIRK/$mGlu_2R$/2AR clones the closest to this ratio observed was 1:1. Crosstalk positive clones were the ones with ratios close to 1:1 whereas higher ratios (2:1 to 4:1) characterized crosstalk-negative clones. The difference between crosstalk positive and crosstalk negative clones became more evident when, in order to account for factors regulating trafficking and/or stability on the cell surface, we introduced the ratio of the "efficiency" of each receptor's mRNA to produce protein that reaches or stays at the cell surface (or $mGlu_2R$/2AR normalized surface protein ratio) which clearly differentiated positive from negative clones. Plotting the normalized $mGlu_2R$ surface protein (surf. protein/mRNA) against the normalized 2AR surface protein

for each clone revealed a clear segregation of crosstalk positive clones to a different area than the one corresponding to the negative ones (Online Resource 4, Fig. S2e, grey and white areas, respectively). Remarkably, clones well within each sub-area (either grey or white) showed a consistent phenotype, either positive (e.g. clones 80 and 106) or negative (e.g. clone 45) in all assays tested, whereas clones close to the borderline between the positive and negative areas (e.g. clones 3 and 92) showed unexpected behaviors. Clone 92 showed an inconsistent behavior in calcium imaging experiments (Online Resource 4, Fig. S2b), but it behaved consistently as a crosstalk positive clone in potentiometric probe assays (Online Resource 4, Fig. S2f) and it showed a crosstalk positive phenotype in terms of the $mGlu_2R/2AR$ normalized surface protein ratio (Online Resource 4, Fig.S2d). Notably, although it classified among the crosstalk positive clones in terms of colocalization of the two receptors, it showed the lowest percentage of colocalization compared to any one of the crosstalk positive clones (Online Resource 4, Fig. S2c, see also Fig. 3c). Clone 3, although it displayed very consistent responses in calcium imaging assays, it showed a unique inverse cross-signaling (Online Resource 4, Fig. S2a) the nature of which is not clear. It seems that, within the range of expression of the two receptors in our clones, clones exhibiting the most consistent cross-signaling are the ones with the highest $mGlu_2R$ and the lowest 2AR normalized surface protein expression (surface protein per RNA unit). This could be either the cause or the consequence of heteromerization. In the most simplified “cause” type of scenarios, too high levels of 2AR for example (always relative to mGlu2R) may favor homomerization versus heteromerization, whereas in the “consequence” type of scenarios, differences in transportation and/or stability between mGlu2R/2AR heteromers and mGlu2R or 2AR homomers may account for differences in each receptor’s normalized expression (surface protein per unit RNA). The above scenarios can become more complicated if one takes into account the possibility of random formation of complexes of “wrong” stoichiometries, with different transportation or stability parameters, compared to either homomers or heteromers of the right stoichiometry. The gap in our current understanding of the critical steps intervening between the relative receptor mRNA expression to the cell surface localization of the $mGlu_2R/2AR$ heterocomplex makes it difficult to discern what exactly is the critical difference between crosstalk positive and crosstalk negative heterocomplexes. What is the subunit stoichiometry of crosstalk positive versus negative heterocomplexes? Are these heterocomplexes preformed and trafficked to the cell surface or can they assemble in a dynamic manner at the cell surface? Regardless of the underlying interesting cell biology that will clarify our understanding of the make-up of cross-signaling heterocomplexes, our study shows that they do exist in mammalian cells and can be differentiated from crosstalk negative heterocomplexes.

A critical result provided by Fribourg et al. both in *Xenopus* oocytes expressing the two receptors at suboptimal RNA ratios and in mice heterozygous for one or the other receptor was the rescue of cross-signaling and its physiological function upon co-administration of ligands for the two receptors whose actions push the Gi-Gq balance in the same direction. Similarly, co-administration of Paliperidone and LY37 also produced significant cross-signaling enhancement in a representative example of HEK293 crosstalk-negative clones compared to an example of crosstalk-positive ones. These results are consistent with our binding demonstrating that crosstalk negative clones, although well differentiated from

crosstalk-positive ones, are clearly different from 2AR homomers, indicating the presence of some level of allosteric interactions. Thus, even crosstalk-negative heterocomplexes can be made to cross-signal given the appropriate stimuli. This is a critical point in the case of schizophrenia, where the relative receptor levels are dysregulated [13] and one may be working mostly with crosstalk-negative heterocomplexes, as assessed by responses to single ligands. Our results suggest that a combination of drugs targeting both receptors may be equally or more efficacious in treating psychosis than higher doses of compounds targeting a single receptor that are plagued with unwanted side effects.

Two months following publication of the evidence for cross-signaling through the $mGlu_2R$/2AR heterocomplex by Fribourg et al. [11], a report by Delille and colleagues appeared online arguing for lack of functional crosstalk evidence in HEK293 cells stably expressing $mGlu_2$ and 2A receptors [6]. Although these authors could detect formation of the $mGlu_2R$/2AR heterocomplex, they challenged the biological relevance of the heterocomplex (also see later review by the same authors [7]. The present study directly responds to this challenge and demonstrates both binding and functional crosstalk between the $mGlu_2$ and 2A receptors. Yet, in the present study only 25–30% of the clonal cells tested showed functional cross-signaling even though all cells were subjected to the same protocol for generation of stable cell lines. It is likely that under the conditions of the relative receptor expression used, the Dellile et al. study predominantly produced crosstalk-negative heterocomplexes. If that were the case, dual administration of a strong agonist/inverse agonist combination for the $mGlu_2R$/2AR heterocomplex would have tested whether cross-signaling could still be observed.

Future development of bivalent ligands able to selectively bind heterocomplexes and not their homomeric counterparts promises to provide useful tools to identify and probe heterocomplex behavior in cellular model systems and *in vivo* animal models. The development of stable cell lines expressing crosstalk-positive and negative $mGlu_2R$/2AR heterocomplexes provides the opportunity to use these cells for high throughput screening of antipsychotic ligands targeting these receptors. The incorporation of a channel reporter in these cell lines and the use of fluorescent potentiometric dyes in our study have shown the feasibility of this approach. Yet in our hands, the FLIPR dye showed batch-to-batch variation in terms of its response to DMSO solvents that could preclude its reliable use to screen water-insoluble drugs that need to be dissolved in DMSO. Better tools will need to be developed to exploit the potential of this system for high throughput screening of antipsychotic agents.

Supplementary Material

Refer to Web version on PubMed Central for supplementary material.

Acknowledgments

The authors wish to thank Dr. Taihao Jin (University of California, San Francisco) for developing an automated program to read fluorescent data from 96-well microplates in a Flex Station 3 reader, Dr Clive M. Baumgarten (Virginia Commonwealth University) for kindly offering access to his patch-clamp rigs, Dr George Liapakis (University of Crete, Greece) for preliminary binding experiments in the clonal cell lines, Drs Carlos A. Villalba-Galea (Virginia Commonwealth University) and Qiong Yao Tang (Xuzhou Medical College, Xuzhou, Jiangsu

Province, CHINA) for help with electrophysiology experiments and Junghoon Ha for analysis and with the presentation of Fig. S3. We also thank all members of the Logothetis lab for critical feedback on the work and the manuscript. We acknowledge Heikki Vaananen and Nada Marjanovic for technical support and the Icahn School of Medicine at Mount Sinai Quantitative PCR Core Facility.

This work was supported by National Institutes of Health grants: R01HL59949 and R01 HL090882 to D.E.L, R01MH084894 to J.G-M and T32 MH096678 training grant to M.F.

References

1. Albizu L, Holloway T, Gonzalez-Maeso J, Sealfon SC. Functional crosstalk and heteromerization of serotonin 5-HT2A and dopamine D2 receptors. Neuropharmacology. 2011; 61:770–777. [PubMed: 21645528]
2. Bezbradica JS, Rosenstein RK, DeMarco RA, Brodsky I, Medzhitov R. A role for the ITAM signaling module in specifying cytokine-receptor functions. Nature immunology. 2014; 15:333–342. [PubMed: 24608040]
3. Borderia AV, Hartmann BM, Fernandez-Sesma A, Moran TM, Sealfon SC. Antiviral-activated dendritic cells: a paracrine-induced response state. Journal of immunology. 2008; 181:6872–6881.
4. Breitwieser GE, Szabo G. Uncoupling of cardiac muscarinic and beta-adrenergic receptors from ion channels by a guanine nucleotide analogue. Nature. 1985; 317:538–540. [PubMed: 2413368]
5. Bulenger S, Marullo S, Bouvier M. Emerging role of homo- and heterodimerization in G-protein-coupled receptor biosynthesis and maturation. Trends in pharmacological sciences. 2005; 26:131–137. [PubMed: 15749158]
6. Delille HK, Becker JM, Burkhardt S, Bleher B, Terstappen GC, Schmidt M, Meyer AH, Unger L, Marek GJ, Mezler M. Heterocomplex formation of 5-HT2A–mGlu2 and its relevance for cellular signaling cascades. Neuropharmacology. 2012; 62:2184–2191. [PubMed: 22300836]
7. Delille HK, Mezler M, Marek GJ. The two faces of the pharmacological interaction of mGlu2 and 5-HT(2)A - relevance of receptor heterocomplexes and interaction through functional brain pathways. Neuropharmacology. 2013; 70:296–305. [PubMed: 23466331]
8. Fell MJ, Svensson KA, Johnson BG, Schoepp DD. Evidence for the role of metabotropic glutamate (mGlu)2 not mGlu3 receptors in the preclinical antipsychotic pharmacology of the mGlu2/3 receptor agonist (−)-(1R,4S,5S,6S)-4-amino-2-sulfonylbicyclo[3.1.0]hexane-4,6-dicarboxylic acid (LY404039). The Journal of pharmacology and experimental therapeutics. 2008; 326:209–217. [PubMed: 18424625]
9. Ferre S, Quiroz C, Orru M, Guitart X, Navarro G, Cortes A, Casado V, Canela EI, Lluis C, Franco R. Adenosine A(2A) Receptors and A(2A) Receptor Heteromers as Key Players in Striatal Function. Frontiers in neuroanatomy. 2011; 5:36. [PubMed: 21731559]
10. Ferre S, Torvinen M, Antoniou K, Irenius E, Civelli O, Arenas E, Fredholm BB, Fuxe K. Adenosine A1 receptor-mediated modulation of dopamine D1 receptors in stably cotransfected fibroblast cells. The Journal of biological chemistry. 1998; 273:4718–4724. [PubMed: 9468534]
11. Fribourg M, Moreno JL, Holloway T, Provasi D, Baki L, Mahajan R, Park G, Adney SK, Hatcher C, Eltit JM, Ruta JD, Albizu L, Li Z, Umali A, Shim J, Fabiato A, MacKerell AD Jr, Brezina V, Sealfon SC, Filizola M, Gonzalez-Maeso J, Logothetis DE. Decoding the signaling of a GPCR heteromeric complex reveals a unifying mechanism of action of antipsychotic drugs. Cell. 2011; 147:1011–1023. [PubMed: 22118459]
12. Gomes I, Gupta A, Filipovska J, Szeto HH, Pintar JE, Devi LA. A role for heterodimerization of mu and delta opiate receptors in enhancing morphine analgesia. Proceedings of the National Academy of Sciences of the United States of America. 2004; 101:5135–5139. [PubMed: 15044695]
13. Gonzalez-Maeso J, Ang RL, Yuen T, Chan P, Weisstaub NV, Lopez-Gimenez JF, Zhou M, Okawa Y, Callado LF, Milligan G, Gingrich JA, Filizola M, Meana JJ, Sealfon SC. Identification of a serotonin/glutamate receptor complex implicated in psychosis. Nature. 2008; 452:93–97. [PubMed: 18297054]
14. Hatcher-Solis C, Fribourg M, Spyridaki K, Younkin J, Ellaithy A, Xiang G, Liapakis G, Gonzalez-Maeso J, Zhang H, Cui M, Logothetis DE. G protein-coupled receptor signaling to kir channels in Xenopus oocytes. Current pharmaceutical biotechnology. 2014; 15:987–995. [PubMed: 25374032]

15. He C, Zhang H, Mirshahi T, Logothetis DE. Identification of a potassium channel site that interacts with G protein betagamma subunits to mediate agonist-induced signaling. The Journal of biological chemistry. 1999; 274:12517–12524. [PubMed: 10212228]
16. Janovick JA, Knollman PE, Brothers SP, Ayala-Yanez R, Aziz AS, Conn PM. Regulation of G protein-coupled receptor trafficking by inefficient plasma membrane expression: molecular basis of an evolved strategy. The Journal of biological chemistry. 2006; 281:8417–8425. [PubMed: 16446355]
17. Jones KA, Borowsky B, Tamm JA, Craig DA, Durkin MM, Dai M, Yao WJ, Johnson M, Gunwaldsen C, Huang LY, Tang C, Shen Q, Salon JA, Morse K, Laz T, Smith KE, Nagarathnam D, Noble SA, Branchek TA, Gerald C. GABA(B) receptors function as a heteromeric assembly of the subunits GABA(B)R1 and GABA(B)R2. Nature. 1998; 396:674–679. [PubMed: 9872315]
18. Jordan BA, Devi LA. G-protein-coupled receptor heterodimerization modulates receptor function. Nature. 1999; 399:697–700. [PubMed: 10385123]
19. Kaupmann K, Malitschek B, Schuler V, Heid J, Froestl W, Beck P, Mosbacher J, Bischoff S, Kulik A, Shigemoto R, Karschin A, Bettler B. GABA(B)-receptor subtypes assemble into functional heteromeric complexes. Nature. 1998; 396:683–687. [PubMed: 9872317]
20. Khalil AM, Cambier JC, Shlomchik MJ. B cell receptor signal transduction in the GC is short-circuited by high phosphatase activity. Science. 2012; 336:1178–1181. [PubMed: 22555432]
21. Kinon BJ, Millen BA, Zhang L, McKinzie DL. Exploratory Analysis for a Targeted Patient Population Responsive to the Metabotropic Glutamate 2/3 Receptor Agonist Pomaglumetad Methionil in Schizophrenia. Biological psychiatry. 2015
22. Knapman A, Santiago M, Du YP, Bennallack PR, Christie MJ, Connor M. A continuous, fluorescence-based assay of mu-opioid receptor activation in AtT-20 cells. Journal of biomolecular screening. 2013; 18:269–276. [PubMed: 23015017]
23. Kobrinsky E, Mirshahi T, Zhang H, Jin T, Logothetis DE. Receptor-mediated hydrolysis of plasma membrane messenger PIP2 leads to K+-current desensitization. Nature cell biology. 2000; 2:507–514. [PubMed: 10934471]
24. Logothetis DE, Kurachi Y, Galper J, Neer EJ, Clapham DE. The beta gamma subunits of GTP-binding proteins activate the muscarinic K+ channel in heart. Nature. 1987; 325:321–326. [PubMed: 2433589]
25. Logothetis DE, Petrou VI, Zhang M, Mahajan R, Meng XY, Adney SK, Cui M, Baki L. Phosphoinositide control of membrane protein function: a frontier led by studies on ion channels. Annual review of physiology. 2015; 77:81–104.
26. Lopez-Gimenez JF, Canals M, Pediani JD, Milligan G. The alpha1b–adrenoceptor exists as a higher-order oligomer: effective oligomerization is required for receptor maturation, surface delivery, and function. Molecular pharmacology. 2007; 71:1015–1029. [PubMed: 17220353]
27. Markey KA, Koyama M, Gartlan KH, Leveque L, Kuns RD, Lineburg KE, Teal BE, MacDonald KP, Hill GR. Cross-dressing by donor dendritic cells after allogeneic bone marrow transplantation contributes to formation of the immunological synapse and maximizes responses to indirectly presented antigen. Journal of immunology. 2014; 192:5426–5433.
28. Moreno JL, Miranda-Azpiazu P, Garcia-Bea A, Younkin J, Cui M, Kozlenkov A, Ben-Ezra A, Voloudakis G, Fakira AK, Baki L, Ge Y, Georgakopoulos A, Moron JA, Milligan G, Lopez-Gimenez JF, Robakis NK, Logothetis DE, Meana JJ, Gonzalez-Maeso J. (Accepted for Publication) Allosteric signaling through an mGlu2 and 5-HT2A heteromeric receptor complex and its potential contribution to schizophrenia. Science Signaling.
29. Moreno JL, Muguruza C, Umali A, Mortillo S, Holloway T, Pilar-Cuellar F, Mocci G, Seto J, Callado LF, Neve RL, Milligan G, Sealfon SC, Lopez-Gimenez JF, Meana JJ, Benson DL, Gonzalez-Maeso J. Identification of three residues essential for 5-hydroxytryptamine 2A–metabotropic glutamate 2 (5-HT2A.mGlu2) receptor heteromerization and its psychoactive behavioral function. The Journal of biological chemistry. 2012; 287:44301–44319. [PubMed: 23129762]
30. Patil ST, Zhang L, Martenyi F, Lowe SL, Jackson KA, Andreev BV, Avedisova AS, Bardenstein LM, Gurovich IY, Morozova MA, Mosolov SN, Neznanov NG, Reznik AM, Smulevich AB, Tochilov VA, Johnson BG, Monn JA, Schoepp DD. Activation of mGlu2/3 receptors as a new

approach to treat schizophrenia: a randomized Phase 2 clinical trial. Nature medicine. 2007; 13:1102–1107.

31. Rao RR, Li Q, Gubbels Bupp MR, Shrikant PA. Transcription factor Foxo1 represses T-bet-mediated effector functions and promotes memory CD8(+) T cell differentiation. Immunity. 2012; 36:374–387. [PubMed: 22425248]
32. Rives ML, Vol C, Fukazawa Y, Tinel N, Trinquet E, Ayoub MA, Shigemoto R, Pin JP, Prezeau L. Crosstalk between GABAB and mGlu1a receptors reveals new insight into GPCR signal integration. The EMBO journal. 2009; 28:2195–2208. [PubMed: 19590495]
33. Ruchala I, Cabra V, Solis E Jr, Glennon RA, De Felice LJ, Eltit JM. Electrical coupling between the human serotonin transporter and voltage-gated Ca(2+) channels. Cell calcium. 2014; 56:25–33. [PubMed: 24854234]
34. Saugstad JA, Segerson TP, Westbrook GL. Metabotropic glutamate receptors activate G-protein-coupled inwardly rectifying potassium channels in Xenopus oocytes. The Journal of neuroscience : the official journal of the Society for Neuroscience. 1996; 16:5979–5985. [PubMed: 8815880]
35. Shen MY, Perreault ML, Fan T, George SR. The dopamine D1-D2 receptor heteromer exerts a tonic inhibitory effect on the expression of amphetamine-induced locomotor sensitization. Pharmacology, biochemistry, and behavior. 2015; 128:33–40.
36. Spooren WP, Gasparini F, van der Putten H, Koller M, Nakanishi S, Kuhn R. Lack of effect of LY314582 (a group 2 metabotropic glutamate receptor agonist) on phencyclidine-induced locomotor activity in metabotropic glutamate receptor 2 knockout mice. European journal of pharmacology. 2000; 397:R1–R2. [PubMed: 10844118]
37. Tang Y, Li X, He J, Lu J, Diwu Z. Real-time and high throughput monitoring of cAMP in live cells using a fluorescent membrane potential-sensitive dye. Assay and drug development technologies. 2006; 4:461–471. [PubMed: 16945018]
38. Vazquez M, Dunn CA, Walsh KB. A fluorescent screening assay for identifying modulators of GIRK channels. Journal of visualized experiments : JoVE. 2012
39. Vilardaga JP, Nikolaev VO, Lorenz K, Ferrandon S, Zhuang Z, Lohse MJ. Conformational crosstalk between alpha2A–adrenergic and mu-opioid receptors controls cell signaling. Nature chemical biology. 2008; 4:126–131. [PubMed: 18193048]
40. Walsh KB. A real-time screening assay for GIRK1/4 channel blockers. Journal of biomolecular screening. 2010; 15:1229–1237. [PubMed: 20938046]
41. Walsh KB. Targeting GIRK Channels for the Development of New Therapeutic Agents. Frontiers in pharmacology. 2011; 2:64. [PubMed: 22059075]
42. White JH, Wise A, Main MJ, Green A, Fraser NJ, Disney GH, Barnes AA, Emson P, Foord SM, Marshall FH. Heterodimerization is required for the formation of a functional GABA(B) receptor. Nature. 1998; 396:679–682. [PubMed: 9872316]
43. Woolley ML, Pemberton DJ, Bate S, Corti C, Jones DN. The mGlu2 but not the mGlu3 receptor mediates the actions of the mGluR2/3 agonist, LY379268, in mouse models predictive of antipsychotic activity. Psychopharmacology. 2008; 196:431–440. [PubMed: 18057917]

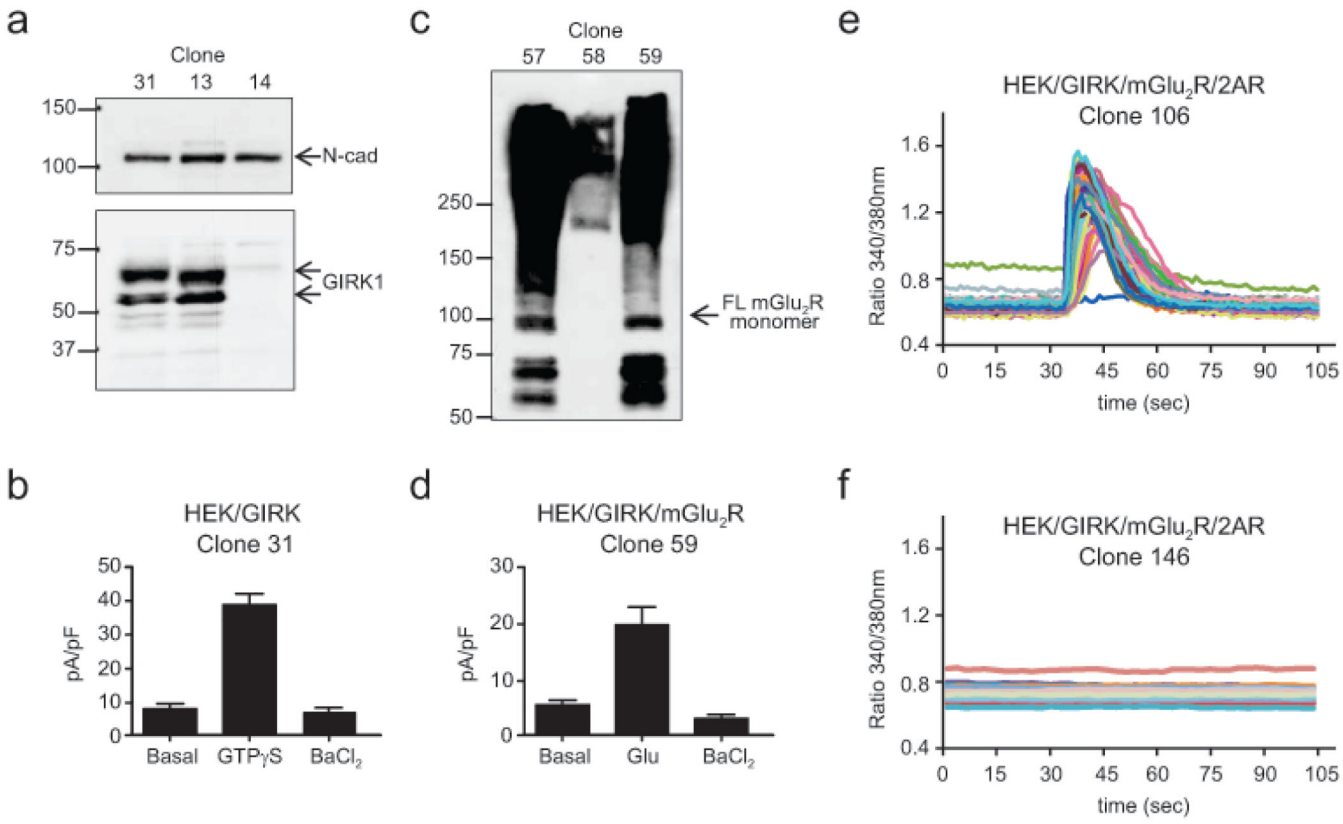

Fig. 1. Generation of HEK/GIRK/mGlu$_2$R/2AR clones

a Western blot analysis of GIRK1 and N-cadherin levels in three puromycin-resistant clones of HEK293 cells transfected with GIRK1+GIRK4 (HEK/GIRK clones). Numbers on the top indicate clone IDs. **b** Summary of data from whole-cell patch-clamp recordings of GIRK activity in HEK/GIRK clone 31 in response to 100 μM GTPγS included in the patch pipette and within a couple of minutes following establishment of the whole-cell recording mode. For each cell, the current was normalized to membrane capacitance and data are expressed as pA/pF. **c** Western blot analysis of mGlu$_2$R levels in three G418-resistant clones of HEK/GIRK cells transfected with HA-mGlu$_2$R. Numbers on the top indicate clone IDs. **d** Summary of data from whole-cell patch clamp recordings of GIRK currents in response to 100 μM Glu in HEK/GIRK/mGlu$_2$R clone 59. Data are expressed as pA/pF. **e, f** Examples of 2AR-positive (**e**) and 2AR-negative (**f**) hygromycin-resistant clones of HEK/GIRK/mGlu$_2$R cells transfected with Myc-2AR. Responses of FURA-2-loaded cells to 10 μM 5-HT were monitored by calcium imaging in an epiluorescence microscope under constant perfusion

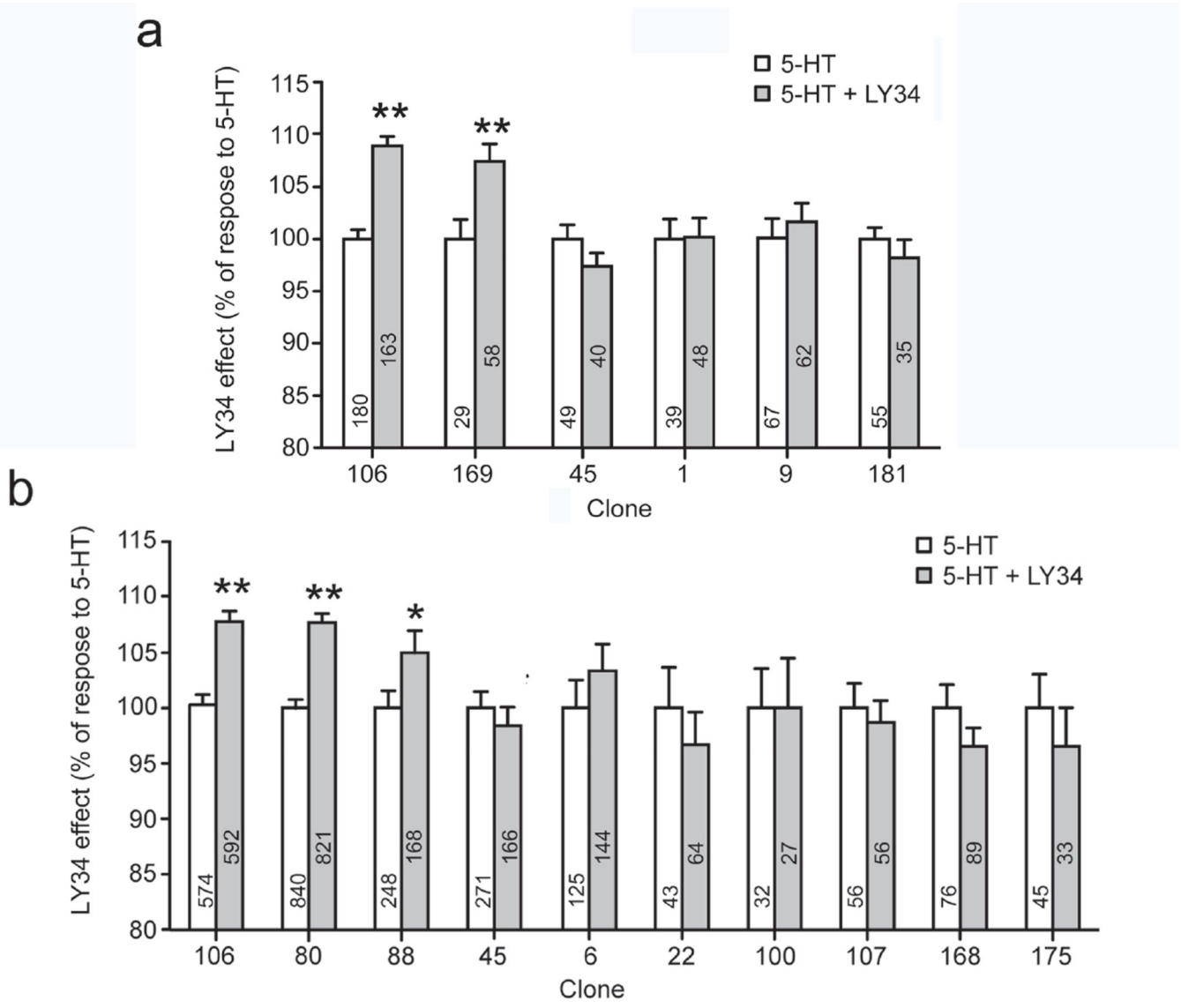

Fig. 2. Effects of the mGlu$_2$R inverse agonist LY34 on serotonin-induced calcium signaling

FURA-2-loaded cells from different HEK/GIRK/mGlu$_2$R/2AR clones were stimulated with either 5-HT (white bars), or 5-HT + LY34 (grey bars). Calcium responses were measured by epifluorescence microscopy under constant perfusion. **a** Summary of responses to 10 μM 5-HT ± 100 μM of LY34. **b** Summary of responses to 20–50 nM 5-HT ± 100 μM of LY34. Data are presented relative to the corresponding responses to 5-HT alone (mean ± S.E.). One asterisk indicates $p \leq 0.05$, two asterisks indicate $p \leq 0.005$. Numbers in the x-axes indicate clone IDs. Numbers inside the bars indicate the number of cells analyzed

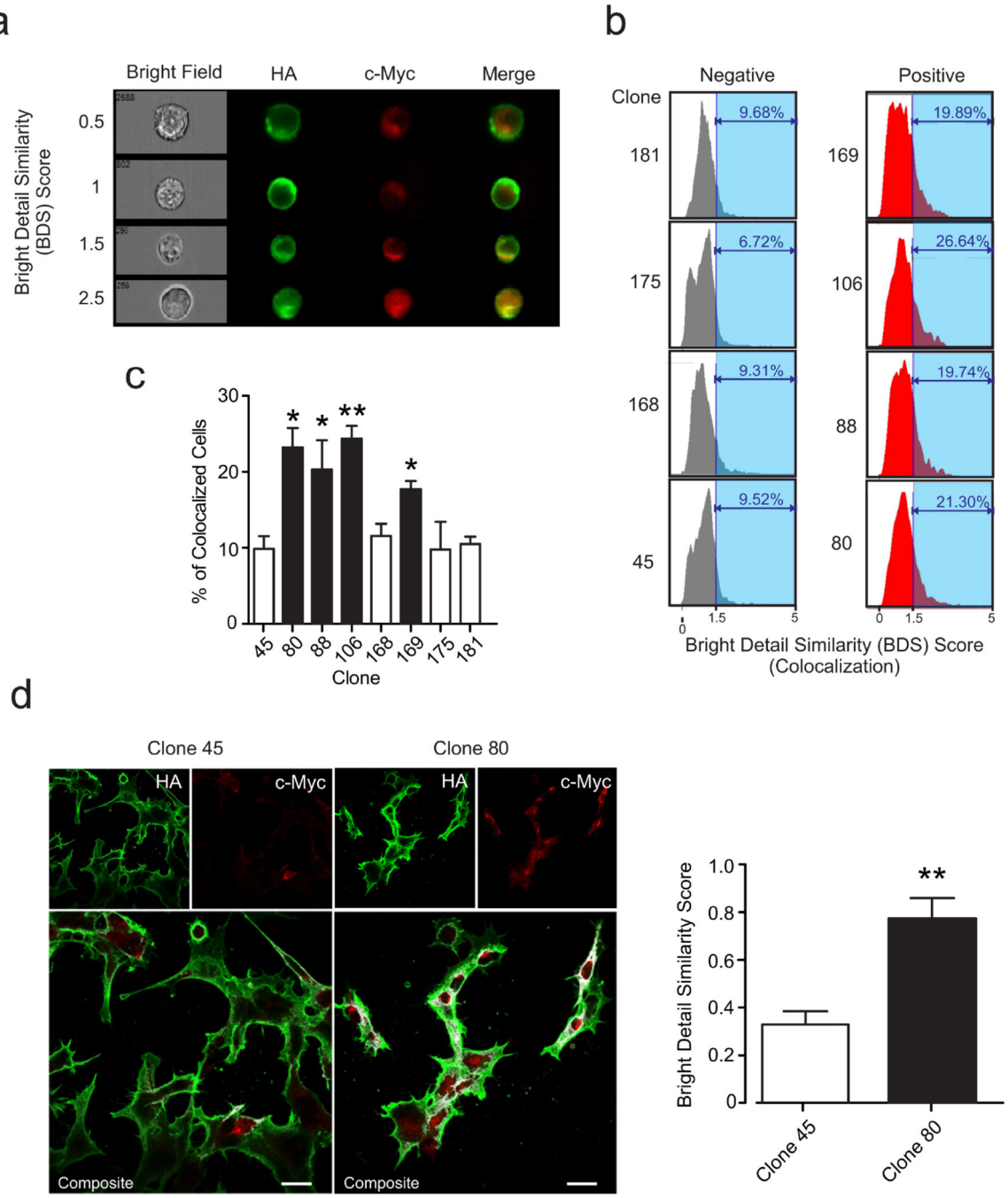

Fig. 3. Cells from crosstalk-positive clones show a higher degree of colocalized signal for mGlu$_2$R and 2AR

a Cells stably transfected with mGlu$_2$R-HA and 2AR-c-Myc were stained with anti-HA and anti-c-Myc antibodies conjugated to fluorophores Alexa Fluor 488 and Alexa Fluor 647, respectively. Images were obtained using Image Stream (AMNIS). In order to quantify colocalization of the mGlu$_2$R-HA and 2AR-c-Myc signals for each cell a Bright Detail Similarity (BDS) score was calculated between the images (see Methods). A negative gate was established using an irrelevant signal (Bright Field). A cell with BDS score greater or

equal to 1.5 was considered to have highly-colocalized signals. The figure shows representative examples of cells where $mGlu_2R$-HA and 2AR-c-Myc signals do not colocalize (BDS scores of 0.5, 1) and colocalize (BDS scores 1.5 and 2.5). **b** Representative ImageStream histograms depicting receptor surface expression in crosstalk-negative (left column, gray) and crosstalk-positive (right column red) clones. **c** Colocalization data for each of the above clones measured by Image Stream (AMNIS). Data are representative of a number of independent experiments N=3–10. One-way ANOVA. * $p<0.05$, ** $p<0.01$. **d** (Left) Representative confocal laser microscopy images of clone 80 (crosstalk-positive) and clone 45 (crosstalk-negative) cells attached and stained with anti-HA and anti-c-Myc antibodies conjugated to fluorophores Alexa Fluor 488 (green) and Alexa Fluor 647 (red) respectively. Composite image indicates in white the colocalization of both signals. Scale bar corresponds to 20 microns. (Right) BDS score calculated between HA and 2AR-c-Myc signals for each image (negative controls with Bright Field images yielded a BDS score average of 0.093). N=9 from two independent experiments. Two-tailed t-test. ** $p<0.01$.

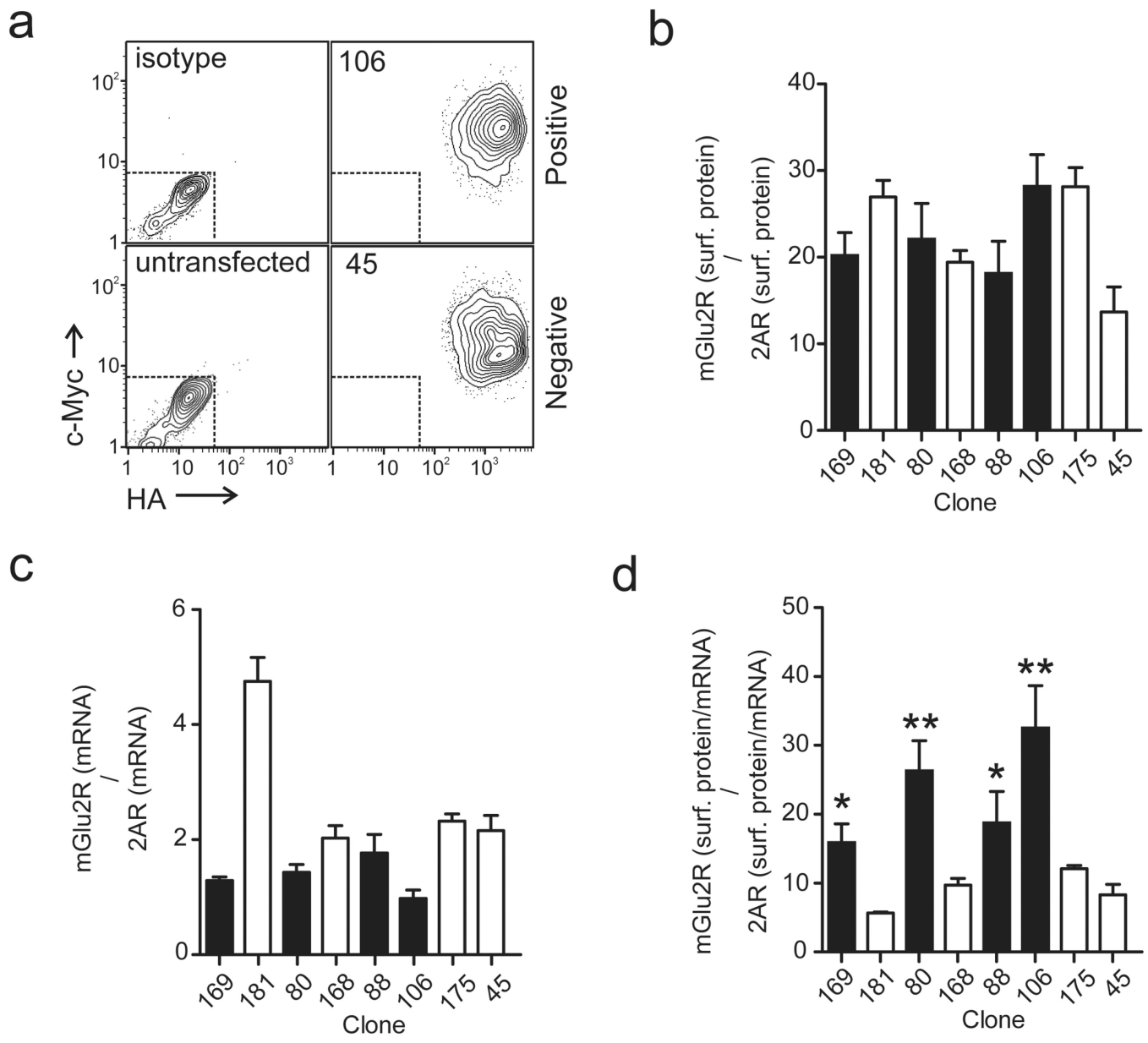

Fig. 4. Differentiation between crosstalk-positive and crosstalk-negative clones based on mGlu$_2$R/2AR surface proteins normalized to their own mRNA

a Representative ImageStream scatter plots depicting receptor surface expression in a crosstalk-positive (clone 106,) and a crosstalk-negative (clone 45) clone stably transfected with mGlu$_2$R-HA and 2AR-cmyc (right panels). Cells were stained with anti-HA and anti-cmyc antibodies conjugated to fluorophores Alexa Fluor 488 and Alexa Fluor 647 respectively. Control scatter plots generated by using either the same set of antibodies in untransfected cells or isotype controls in transfected cells are shown in the left panels. **b** Ratios of mGlu$_2$R/2AR surface protein in crosstalk-positive (filled bars) and crosstalk-negative clones (open bars), as determined by flow cytometry using immunofluorescence. Cells were stained with anti-HA anti-cMyc antibodies conjugated to fluorophores Alexa Fluor 488 and Alexa Fluor 657, respectively. **c** Ratios of mGlu$_2$R/2AR mRNA in crosstalk

positive (filled bars) and crosstalk negative clones (open bars) as determined by RT-PCR. **d** Surface protein expression for each receptor was normalized to its respective mRNA. Ratios of normalized (protein/mRNA) $mGlu_2R$ to normalized (protein/mRNA) 2AR are shown for crosstalk-positive (filled bars) and crosstalk negative (open bars) clones. Data are representative of a number of independent experiments N=3–10. One-way ANOVA. * $p<0.05$, ** $p<0.01$

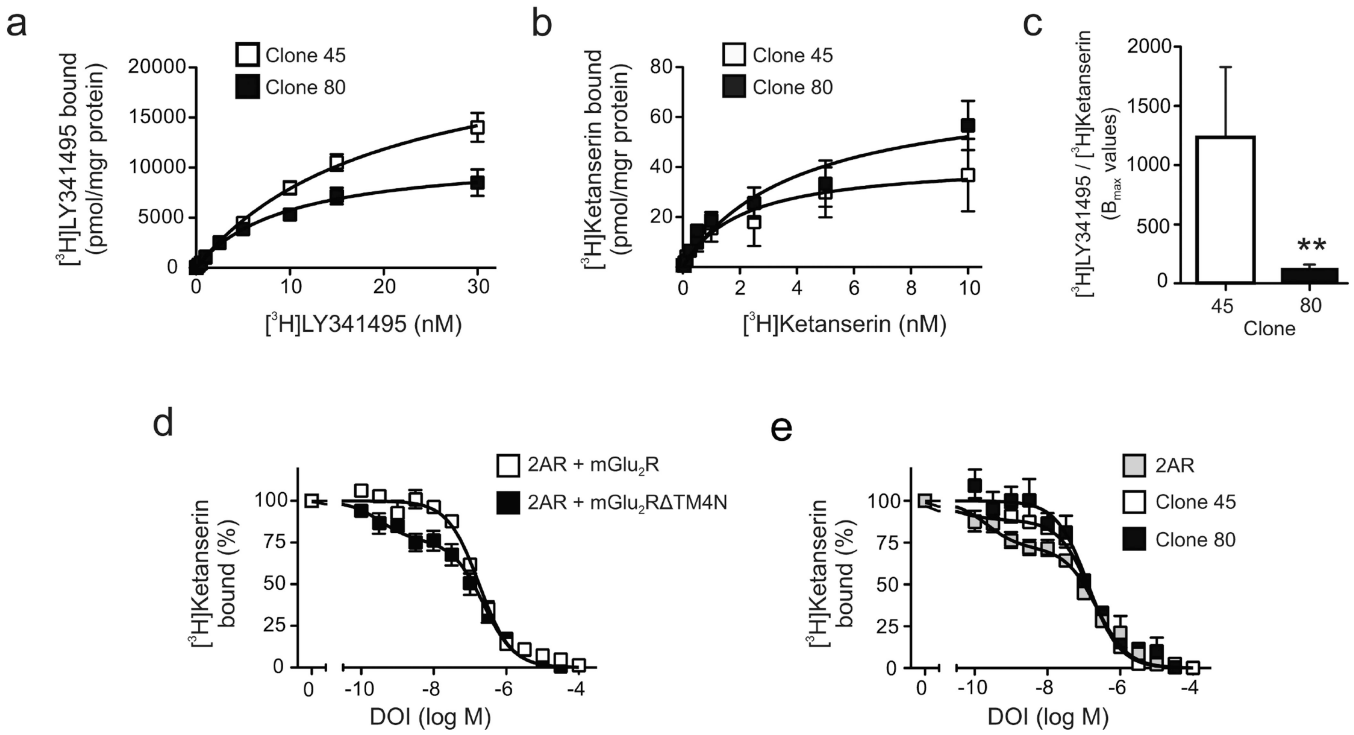

Fig. 5. Allosteric crosstalk between 2AR and $mGlu_2R$ in clone 45 and clone 80

a [^{3}H]LY341495 binding saturation curves in plasma membrane preparations of clones 45 and 80. The best-fit values differ between clone 45 and clone 80 ($F[2,95] = 49.74$; $p < 0.001$; $n = 4–5$). **b** [^{3}H]Ketanserin binding saturation curves in total membrane preparations of clones 45 and 80. The best-fit values differ between clone 45 and clone 80 ($F[2,136] = 3.13$; $p < 0.05$; $n = 4$). **c** Ratios of [^{3}H]LY341495/[^{3}H]Ketanserin B_{max} values in clones 45 and 80. **d, e** [^{3}H]Ketanserin binding displacement curves by DOI in HEK293 cells co-transfected with 5-HT_{2A} and $mGlu_2$ or $mGlu_2\Delta TM4N$ ($mGlu_{2/3}R$ chimeric construct that does not form the 2AR-$mGlu_2R$ heteromeric complex), or mock (pcDNA3.1), or in clones c45 and c80 ($n = 3–4$). Note that the 2AR affinity for DOI was decreased by $mGlu_2R$, and unaffected by $mGlu_2\Delta TM4N$, assessed by F test. Note that 2AR affinity for DOI in clone 80 is not different to that observed in HEK293 cells co-transfected with 2AR and $mGlu_2R$, assessed by F test. Note also that whereas a two-site model provided a better description for the [^{3}H]Ketanserin binding displacement curves by DOI in clone 45, the best-fit values differ between clone 45 and HEK293 cells transfected with 5-HT_{2A} alone, assessed by F test (see also Table 1)

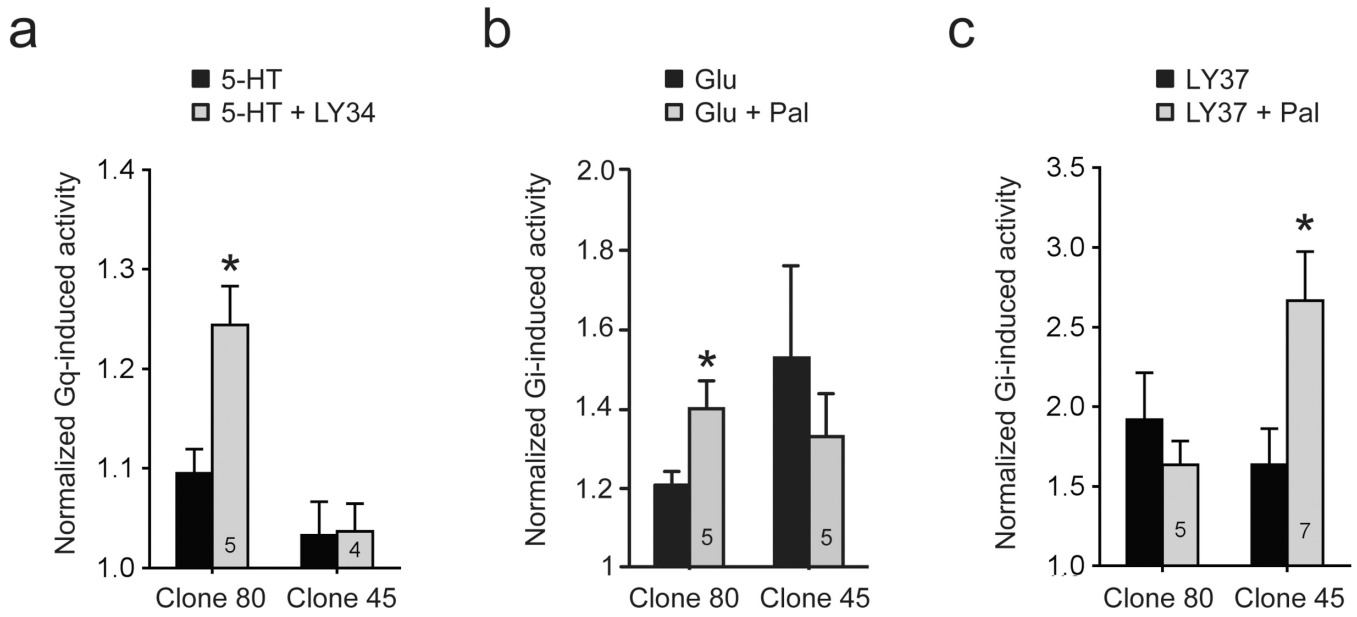

Fig. 6. Cross-signaling between $mGlu_2R$ and 2AR in HEK/GIRK/$mGlu_2R$/2AR cells demonstrated by changes in GIRK channel activity

(a), (b), (c) Summary data from whole-cell patch-clamp recordings of GIRK currents in two clones of HEK/GIRK/$mGlu_2R$/2AR cells exposed to: **a** 5-HT (20 nM), followed by 5-HT (20 nM) + LY34 (100 μM), **b** Glutamate (Glu, 500 nM), followed by Glu (500 nM) + Paliperidone (100 μM) (Glu+Pal), **c** LY37 (50 nM), followed by LY37 (50 nM) + paliperidone (100 μM). Gq activity (A) was measured as GIRK current inhibition. Gi activity **b,c** was measured as GIRK current activation, see Experimental Procedures. Data were normalized to basal activity and results are expressed as mean ±SEM. One asterisk indicates $p \leq 0.05$, two asterisks indicate $p \leq 0.005$. Numbers inside the bars indicate the number of experiments

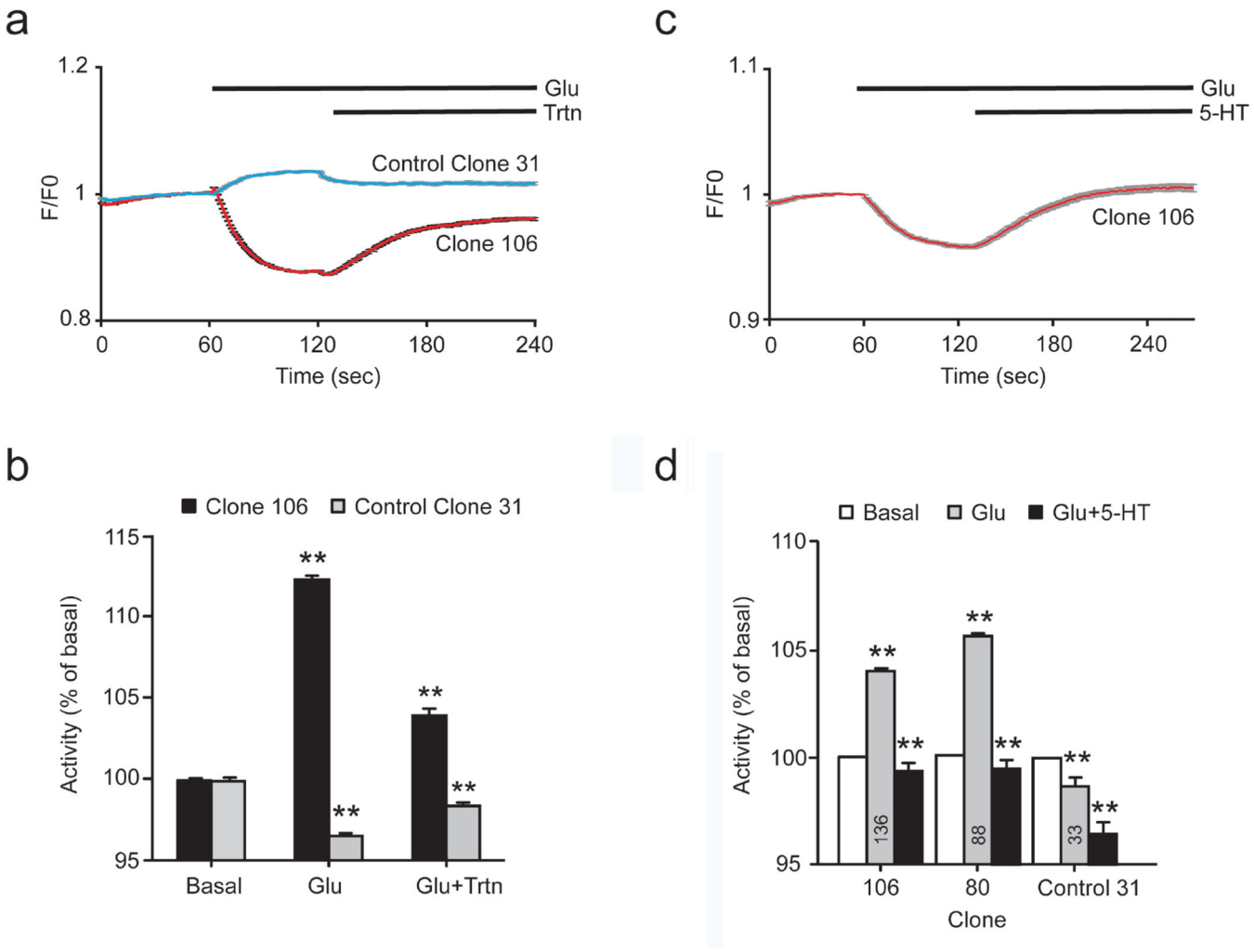

Fig. 7. The potentiometric dye HLB 021–152 reports Gi- and Gq- dependent changes in GIRK channel activity

Responses of HLB 021-152- loaded cells to different drugs were assayed by epifluorescence microscopy under constant perfusion. Traces for each cell were normalized for the mean basal fluorescence of this cell, before addition of the drugs (baseline signal, or F_0). **a** Normalized traces (F/F_0) of responses of cells from the HEK/GIRK/mGlu_2R/2AR clone 106 and from the HEK/GIRK clone 31 to sequential application of Glu (50 μM) followed by Glu + Tertiapin Q (100nM). **b** Summary data from 107 cells from the HEK/GIRK/mGlu_2R/2AR clone 106 and 105 cells from the HEK/GIRK clone 31, presented as % changes in GIRK channel activity (± SEM). Statistical significance for responses to Glu was calculated relative to basal. Statistical significance for responses to Glu+Trtn was calculated relative to Glu alone, ** $p<0.005$. **c** Normalized traces (F/F_0) of responses of cells from the HEK/GIRK/mGlu_2R/2AR clone 106 to sequential application of Glu (50 μM) and Glu and 5-HT (1 μM). **d** Summary data from similar experiments, using cells from two clones of HEK/GIRK/mGlu_2R/2AR and from HEK/GIRK clone 31 (control 31), expressed as changes in GIRK channel activity ± SEM. Clone IDs are shown below the bars; numbers inside the bars indicate the number of cells tested. Statistical significance for responses to Glu was

calculated relative to basal. Statistical significance for responses to Glu+5-HT was calculated relative to Glu alone, ** $p<0.005$

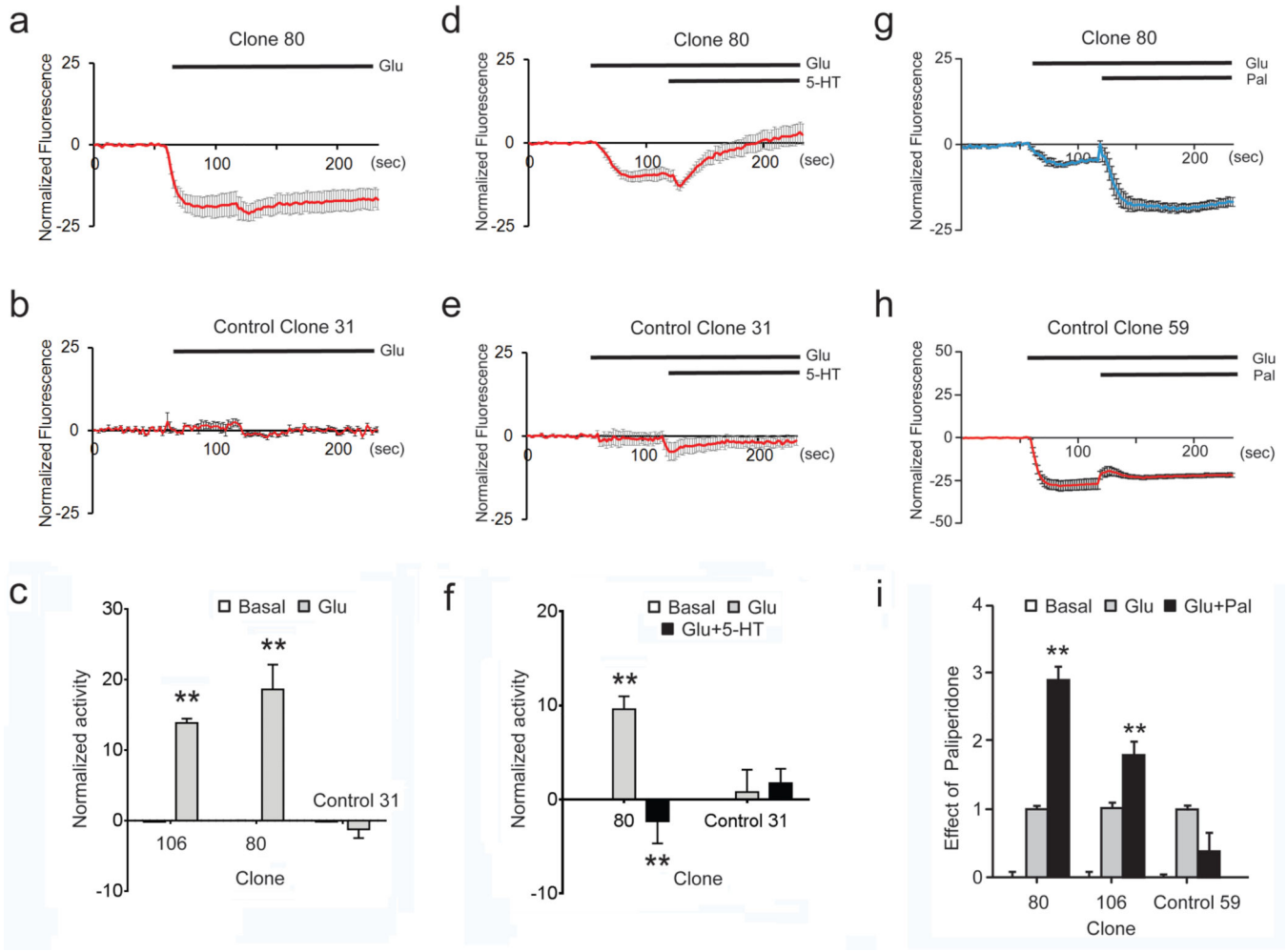

Fig. 8. Cross-signaling responses reported by the potentiometric dye FLIPR Blue

Responses of FLIPR Blue- loaded cells to different drugs were assayed in an automated liquid handling microplate reader. Traces of fluorescent signals were normalized for the mean basal fluorescence and further normalized by subtraction of the changes produced by vehicle addition in control wells (see Methods). **a,b** Normalized traces of responses of cells from HEK/GIRK/mGlu$_2$R/2AR clone 106 (A) and HEK/GIRK clone 31 (B) to Glu (50 μM). **c** Summary of responses to Glu, in clones 106 (N=4), 80 (N=3), and the parental clone 31(N=5), expressed as normalized channel activity (± SEM). ** $p<0.005$ **d,e** Normalized traces of responses of cells from the HEK/GIRK/mGlu$_2$R/2AR clone 80 (D) and HEK/GIRK clone 31 (E) to application of Glu (50 μM), followed by addition of 5-HT (1 μM). **f** Summary of data from clone 80 (N=5), and the parental clone 31 (N=5), expressed as normalized channel activity (± SEM). Statistical significance for responses to Glu was calculated relative to basal. Statistical significance for responses to Glu+5-HT was calculated relative to Glu alone, ** $p<0.005$. **g,h** Normalized traces of responses of cells from HEK/GIRK/mGlu$_2$R/2AR clone 80 **(g)** and the parental clone HEK/GIRK/mGlu$_2$R-59 **(h)** to application of Glu (20 μM), followed by addition of Paliperidone (50 μM). **i** Summary data, obtained using clones 80 (N=19), 106 (N=16), and the parental clone HEK/GIRK/

$mGlu_2R$-59 (N=16), presented relative to the corresponding responses to Glu alone (± SEM). One asterisk indicates $p \leq 0.05$, two asterisks indicate $p \leq 0.005$

Table 1

[^{3}H]Ketanserin binding displacement curves by DOI

Constructs/clones	$K_{i\text{-}high}$ (log M)	$K_{i\text{-}low}$ (log M)	% High
5-HT$_{2A}$	−9.66 ± 0.24	−6.89 ± 0.09	28.11 ± 3.3
5-HT$_{2A}$ + mGlu$_2$	N.A.	7.01 ± 0.04	N.A.
5-HT$_{2A}$ + mGlu$_2$ΔTM4N	−9.48 ± 0.25	−6.88 ± 0.07	23.72 ± 3.1
c45	−10.59 ± 0.51	−7.06 ± 0.01	11.40 ± 1.7
c80	N.A.	−7.13 ± 0.06	N.A.

DOI displacement of [^{3}H]ketanserin (2 nM) binding was performed in HEK293 cells co-transfected with 5-HT$_{2A}$ and mGlu$_2$ or mGlu$_2$ΔTM4N, or mock (pcDNA3.1), or in clones c45 and c80. Competition curves were analyzed by nonlinear regression analysis to derive dissociation constants for high ($K_{i\text{-}high}$) and low ($K_{i\text{-}low}$) affinity states of the receptor. % High refers to the percentage of high affinity binding sites as calculated from nonlinear fitting. Values are best-fit ± S.E. of three or four experiments performed in triplicate. One- or two-site model as a better description of the data was determined by F test. Two-site model, $p < 0.05$. N.A., two-site model not applicable, $p > 0.05$. The best-fit values differ between HEK293 cells transfected with 5-HT$_{2A}$ and clone c45 ($F[3,92] = 7.02$; $p < 0.001$). The best-fit values do not differ between HEK293 cells co-transfected with 5-HT$_{2A}$ and mGlu$_2$ and clone c80 ($F[1,82] = 2.62$; $p > 0.05$)